Speciation in human blood of Metvan, a vanadium based potential anti-tumor drug

Speciation in human blood of Metvan, a vanadium based potential anti-tumor drug

Daniele Sanna,[a] Valeria Ugone,[b] Giovanni Micera,[b] Péter Buglyó,[c] Linda Bíró,[c] Eugenio Garribba,*[b]

[a] *Istituto CNR di Chimica Biomolecolare, Trav. La Crucca 3, I-07040 Sassari, Italy*

[b] *Dipartimento di Chimica e Farmacia, Università di Sassari, Via Vienna 2, I-07100 Sassari, Italy. E-mail: garribba@uniss.it; Tel: +39 079 229487.*

[c] *Department of Inorganic and Analytical Chemistry, University of Debrecen, H-4032 Debrecen, Egyetem tér 1, Hungary*

† Electronic Supplementary Information (ESI) available: concentration distribution curves of the species formed in the systems $V^{IV}O^{2+}$/Me_2phen 1/5 (Fig. S1) and $V^{IV}O^{2+}$/Me_2phen/MeIm 1/5/4 (Fig. S15); anisotropic EPR spectra recorded in the systems $V^{IV}O^{2+}$/Me_2phen 1/5 as a function of pH (Fig. S2), $V^{IV}O^{2+}$/Me_2phen/H_3citr 1/2/2 (Fig. S8), $V^{IV}O^{2+}$/Me_2phen/Hlact 1/2/4 (Fig. S13) and $V^{IV}O^{2+}$/Me_2phen/Hb 2/4/1 and 2/10/1 at pH 7.4 (Fig. S16); positive ESI-MS spectrum recorded in the systems $V^{IV}O^{2+}$/Me_2phen 1/2 and simulated isotopic pattern for the most important peaks (Figs. S3-S6); negative ESI-MS spectrum recorded in the system $V^{IV}O^{2+}$/Me_2phen/H_3citr 1/2/2 and simulated isotopic pattern for the most important peak (Figs. S9 and S10); positive ESI-MS spectrum recorded in the system $V^{IV}O^{2+}$/Me_2phen/H_3citr 1/2/2 and simulated isotopic pattern for the most important peak (Fig. S12); simulated isotopic pattern for the most important peak revealed in the system $V^{IV}O^{2+}$/Me_2phen/Hlact 1/2/4 (Fig. S14); negative ESI-MS/MS spectra recorded in the systems $V^{IV}O^{2+}$/Me_2phen 1/2 (Fig. S7) and $V^{IV}O^{2+}$/Me_2phen/H_3citr 1/2/2 (Fig. S11).

Abstract

The first report on the anti-cancer activity of the compound Metvan, $[V^{IV}O(Me_2phen)_2(SO_4)]$, where Me_2phen is 4,7-dimethyl-1,10-phenanthroline, dates back to 2001. Despite that it was immediately identified as one of the most promising multitargeted anti-cancer V compounds, no development on the medical experimentation was carried out. One of the possible reasons is the lack of information on its speciation in aqueous solution and thermodynamic stability, factors which influence the transport in the blood and the final form which reaches the target organs. To fill this gap, in this work the speciation of Metvan in aqueous solution and human blood was studied by instrumental (EPR, electronic absorption spectroscopy, ESI-MS and ESI-MS/MS), analytical (pH-potentiometry) and computational (DFT) methods. The results suggested that Metvan transforms at physiological pH into the hydrolytic species *cis*-$[VO(Me_2phen)_2(OH)]^+$ and that both citrate and proteins (transferrin, albumin in the blood serum and hemoglobin in the erythrocytes) form mixed complexes, denoted with $[VO(Me_2phen)(citrH_{-1})]^{2-}$ and VO–Me_2phen–Protein with the probable binding of His-N donors. The measurements with erythrocytes suggest that Metvan is able to cross their membrane forming mixed species VO–Me_2phen–Hb. The redox stability in cell culture medium was also examined, showing that *ca*. 60% is oxidized to V^V after 5 h. Overall, the speciation of Metvan in the blood mainly depends on the V concentration: when it is larger than 50 μM $[VO(Me_2phen)(citrH_{-1})]^{2-}$ and VO–Me_2phen–Protein are the major species, while for concentrations lower than 10 μM (VO)(hTf) is formed and Me_2phen is lost. Therefore, it is plausible that the pharmacological activity of Metvan could be due to the synergic action of free Me_2phen, and $V^{IV}O$ and V^VO/V^VO_2 species.

1. Introduction

The possible application of vanadium (V) complexes in medicine has gained a growing interest in the literature over the last years. The first evidence of the anti-diabetic action of a V compound, $NaV^{V}O_3$, dates back to 1899,[1] but more than 80 years went by before this discovery was confirmed.[2] Now, two V^{IV} species, bis(maltolato)oxidovanadium(IV) (BMOV) and bis(ethylmaltolato)oxido-vanadium(IV) (BEOV), are the benchmark complexes for the new molecules with anti-diabetic action.[3] BEOV arrived to phase IIa of the clinical trials,[4] even if these have provisionally been abandoned due to renal problems arising with several patients.[5, 6] Meanwhile, V complexes have been tested and proposed as anti-parasitic, spermicidal, anti-viral, anti-HIV and anti-tuberculosis agents.[5, 7]

In parallel with the study on the anti-diabetic activity, many studies have been devoted to the potential therapeutical application of vanadium in the treatment of cancer.[8] The first report on the potential anti-tumor action of a V compound, bis(η^5-cyclopentadienyl)vanadium(IV) dichloride or vanadocene dichloride (VDC), active in the treatment of Ehrlich ascites tumor, has been published in 1983,[9] and bis-[(*p*-methoxybenzyl)cyclopentadienyl]vanadium(IV) dichloride (vanadocene **Y**) exhibits an IC_{50} value of 3.0 μM against the LLC-PK (pig kidney epithelial) cell line, slightly more active than the 'classic' cisplatin which has an IC_{50} of 3.3 μM.[10] Recently, *in vitro* experiments on vanadocene **Y** di-isoselenocyanate, have shown impressive cytotoxic effects against the human renal cancer cells CAKI-1, with an IC_{50} value reaching for the first time the nanomolar range for a metallocene type drug with anti-cancer potential.[11]

In 2001, the compound $[V^{IV}O(Me_2phen)_2(SO_4)]$, where Me_2phen is 4,7-dimethyl-1,10-phenanthroline (now known as Metvan), was identified as one of the most promising multitargeted anti-cancer V compounds with apoptosis-inducing activity. It was found that it is effective against acute lymphoblastic leukemia (ALL; NALM-6 and MOLT-3), acute myeloid leukemia (AML; HL-60), Hodgkin's disease (HS445), and multiple myeloma (ARH-77, U266BL, and HS-SULTAN) cell lines.[12] Metvan also induces apoptosis in solid tumor cells derived from glioblastoma, breast cancer, ovarian, prostate and testicular cancer patients at a level of nanomolar or low micromolar concentration. For human malignant glioblastoma and breast cancer, Metvan shows delayed tumor progression and increased survival time in models of severe combined immunodeficient mouse xenograft.[7e] Another great advantage over other metal based drugs with antiproliferative potential could be the activity against cisplatin-resistant ovarian and testicular cancer.[8e, 12-13, 14] In spite of these promising and multitargeted anti-cancer actions, no medical experimentation was carried out recently. As pointed out recently in the literature,[15] the reason can be related to the lack of information on its speciation in aqueous solution and its thermodynamic/redox stability, which

influence the transport in the blood and the final form which reaches the target organs, and the identification of the species which promote the intracellular signaling pathways.[16] Indeed, the mechanism of action of Metvan is not yet completely clear. On the one hand it has been stated that – similarly to other V species [17]–, this could be related to the generation of ROS and depletion of glutathione together with a loss of mitochondrial transmembrane potential,[7e] on the other that the aromatic system of Me_2phen may interact with DNA via intercalation and π···π interaction, deactivating DNA and inhibiting cell proliferation.[7c] Recently, most of the observed biological activity of Metvan was related to the free phenanthroline derivative generated in the organism after the dissociation of the complex;[18] in this regard, the examination of the stability at the physiological conditions is of fundamental importance.

In general, when the effectiveness and potential medical application of a metal compound (Metvan in this case) is considered, information on species distribution is necessary because different V complexes have different effects in biological systems;[19] the assumption that V compounds reach the target cells in the same form as they are administrated can be considered as an oversimplification.[19-20] In fact, in the blood – depending on the thermodynamic stability of the specific V compound – ligand exchange, complexation and/or redox reactions can occur and the proteins of the plasma, such as transferrin (hTf), albumin (HSA) and immunoglobulin (Ig), together with the low molecular mass (l.m.m.) bioligands, such as oxalate, lactate, phosphate, citrate or amino acids can interact with the V compound administered and partly or fully displace the organic ligand L.[21, 22, 23, 24] This was demonstrated for another important vanadium compound with potential anti-tumor activity, VDC,[25] and – more in general – for other V containing drugs.[23] In the cellular environment other bioligands, for example glutathione and ascorbate, could replace the organic ligand or promote redox reactions.[26, 27]

With regard to Metvan, Rehder wrote that it is not likely to survive *in vivo* conditions and that the active species could be a simple $V^{IV}O^{2+}$ compound, formed upon the interaction with the plasma and cytosol bioligands.[28] Crans and Lay observed that solubilization of Metvan in cell culture medium led to rapid oxidation of V^{IV} to V^{V} and release of the free ligand, to which the pharmacological activity should be attributed.[18, 29]

Finally, Metvan can distribute between plasma and erythrocytes,[30, 31] and this phenomenon has two possible consequences: i) if an equilibrium between the concentrations of the metal drug in the plasma and red blood cells is reached, the metal complex can be excreted by the erythrocytes and enter the target cells, keeping pharmacological effects (in this case, the erythrocytes would contribute only to the transport of the compound); ii) the metal complex could be 'confined' in the

red blood cells in an inactive form (and this amount would not contribute to the pharmacological effects).[30a]

In this work, all these aspects were examined. In particular, the behavior of Metvan in aqueous solution and its interaction with lactate and citrate (the two l.m.m. bioligands of the plasma with the highest affinity for $V^{IV}O^{2+}$ ion [21a]) and the proteins of the plasma and red blood cells (apo-transferrin, holo-transferrin, albumin, and hemoglobin), and the oxidation process in the cell culture medium were studied. The techniques used were EPR (Electronic Paramagnetic Resonance) and electronic absorption spectroscopy, ESI-MS (ElectroSpray Ionization-Mass Spectrometry), ESI-MS/MS (ElectroSpray Ionization-Tandem Mass Spectrometry), pH-potentiometry and DFT (Density Functional Theory) calculations. The results of this study could allow getting important and new insights in the comprehension of the biospeciation of Metvan in the plasma and erythrocytes and in the identification of the active species under physiological conditions. We hope that the presented results could stimulate new research and discussion in the literature with a view to restart the clinical experimentation on Metvan.

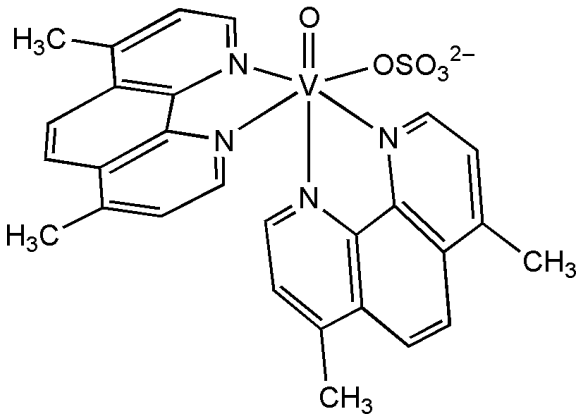

Scheme 1. Structure of $[V^{IV}O(Me_2phen)_2(SO_4)]$ or Metvan.

2. Experimental and Computational Section

2.1. Chemicals

Oxidovanadium(IV) sulfate trihydrate ($VOSO_4 \cdot 3H_2O$), 4,7-dimethyl-1,10-phenanthroline (Me_2phen), 4-(2-hydroxyethyl)piperazine-1-ethanesulfonic acid (HEPES), sodium hydrogen carbonate ($NaHCO_3$), citric acid (H_3citr), lactic acid (Hlact), 1-methylimidazole (MeIm),

ammonium carbonate ($(NH_4)_2CO_3$), sodium chloride (NaCl), sodium dihydrogen phosphate (NaH_2PO_4) and glucose were products Sigma-Aldrich or Fluka of the highest grade available and used as received. Human serum apo-transferrin (apo-hTf, T4283), human serum holo-transferrin (holo-hTf, T4132), human serum albumin (HSA,97-99%, A9511) and hemoglobin (Hb, H7379) were purchased from Sigma-Aldrich with molecular mass of 76-81 kDa, 76-81 kDa, 66 kDa and 64.5 kDa, respectively.

2.2. Preparation of the solutions and EPR measurements

The solutions were prepared dissolving in ultrapure water, obtained through the purification system Millipore MilliQ Academic, a weighted amount of $VOSO_4 \cdot 3H_2O$ and Me_2phen to obtain a metal ion concentration in the range 5.0×10^{-4}–1.0×10^{-3} M and a ligand to metal molar ratio of 2 or 5. The solutions of Metvan were freshly prepared before each experiment because they are not stable and tend to oxidize to V^V.[29] In the ternary systems citric or lactic acid or 1-methylimidazole were added to obtain a ratio $V^{IV}O^{2+}$/Me_2phen/citrate of 1/2/2, $V^{IV}O^{2+}$/Me_2phen/lactate of 1/2/4, and $V^{IV}O^{2+}$/Me_2phen/MeIm of 1/2/4 or 1/5/4. The solutions were bubbled with argon in order to avoid the oxidation of the metal ion.

In the experiments with apo-hTf and holo-hTf, the pH of the solutions containing $V^{IV}O^{2+}$ and Me_2phen was raised to *ca*. 4.0 and $NaHCO_3$ and HEPES were added in appropriate amounts in order to have concentration of 2.5×10^{-2} and 1.0×10^{-1} M, respectively; subsequently, pH was brought to *ca*. 5.0 and apo-hT or holo-hTf were added, pH was increased up to 7.40 and EPR spectra were immediately measured. The final ratio $V^{IV}O^{2+}$/Me_2phen/apo-hTf or $V^{IV}O^{2+}$/Me_2phen/holo-hTf was 2/4/1 or 2/10/1 with a protein concentration of 2.5×10^{-4} M. In the experiments with HSA and Hb an analogous procedure was used, according to the methods established in the literature, with the difference that $NaHCO_3$ was not added.[21b, 30a] The final ratio $V^{IV}O^{2+}$/Me_2phen/HSA and $V^{IV}O^{2+}$/Me_2phen/Hb were 4/8/1 or 4/20/1 (HSA) and 2/4/1 or 2/10/1 (Hb) with a protein concentration of 2.5×10^{-4} M (HSA) and 3.1×10^{-4} M (Hb).

2.3. Preparation of the solutions for ESI-MS measurements

ESI-MS measurements were carried out on the systems $V^{IV}O^{2+}$/Me_2phen, $V^{IV}O^{2+}$/Me_2phen/H_3citr, $V^{IV}O^{2+}$/Me_2phen/Hlact and $V^{IV}O^{2+}$/Me_2phen/MeIm at various pH (4-7) and V concentration (from 2.5×10^{-6} to 1.0×10^{-5} M). The solutions containing $V^{IV}O^{2+}$, Me_2phen and the eventual third ligand were prepared in LC-MS ultrapure water (from Sigma-Aldrich), pH eventually was varied with $(NH_4)_2CO_3$ and ESI-MS or ESI-MS/MS spectra recorded immediately.

2.4. Potentiometric measurements

Protonation constants of the ligands and stability constants of their $V^{IV}O^{2+}$ complexes were determined by pH-potentiometric titrations on 15.00 mL of samples at 25.0 ± 0.1 °C and at a constant ionic strength of 0.20 M (KCl). The $V^{IV}O^{2+}$ concentration was in the range 0.5-4.0 × 10^{-3} M, while for the ternary systems $V^{IV}O^{2+}$/L/H_3citr (H_3B), $V^{IV}O^{2+}$/L/Hlact (HB), and $V^{IV}O^{2+}$/L/MeIm (HB) 1:1:1, 1:2:1, 1:2:2, 1:2:4 and 1:1:4 molar ratios were used. All of the titrations were performed over the pH range 2.0-11.0, or until precipitation occurred with a carbonate-free KOH of known concentration (*ca*. 0.2 M) under a purified argon atmosphere.[32] A Mettler Toledo T50 titrator equipped with a combined glass electrode (type 6.0234.100) was used for the pH-metric measurements. The electrode system was calibrated according to Irving *et al.*,[33] and therefore the pH-metric readings were converted into hydrogen ion concentration. The water ionization constant, pK_w, was 13.76 ± 0.01 under the conditions employed. The reproducibility of the points included in the evaluation was within 0.005 pH unit in the whole pH range measured. The number of experimental points used in the calculations was about 150-250. The stability of the complexes, reported as the logarithm of the overall formation constant $\beta_{pqrs} = [(VO)_pL_qB_rH_s]/[VO]^p[L]^q[B]^r[H]^s$, where VO stands for $V^{IV}O^{2+}$ ion, L and B are the deprotonated forms of Me_2phen and ligand B ($citr^{3-}$, $lact^-$, MeIm) was calculated with the aid of the PSEQUAD program.[34] The stability constants for the species formed in the $V^{IV}O^{2+}$/Me_2phen, $V^{IV}O^{2+}$/H_3citr, $V^{IV}O^{2+}$/Hlact, and $V^{IV}O^{2+}$/MeIm systems were used as fixed values to estimate those of the ternary complexes. The notation H_{-1} indicates proton dissociation of groups which do not deprotonate in the lack of $V^{IV}O^{2+}$ coordination (–OH group of lactate and citrate), or hydroxido ligands. The uncertainties (3σ values) of the stability constants are given in parentheses. During the calculations the following hydroxido complexes of $V^{IV}O^{2+}$ were assumed: $[VO(OH)]^+$ ($\log\beta_{100-1} = -5.94$), $[(VO)_2(OH)_2]^{2+}$ ($\log\beta_{200-2} = -6.95$), with stability constants calculated from the data of Henry *et al.* [34] and corrected for the different ionic strengths by use of the Davies equation,[35] $[VO(OH)_3]^-$ ($\log\beta_{100-3} = -18.0$) and $[(VO)_2(OH)_5]^-$ ($\log\beta_{200-5} = -22.0$).[36, 37]

2.5. Experiments with red blood cells and cell culture medium

Blood samples were obtained from Servizio Trasfusionale Aziendale (AOU of Sassari) and were collected with Vacutest Kima serum separator tubes containing micronised silica particles, which have the role of accelerate clotting (clot activator), and a gel (present in the bottom of the tube), which forms a barrier to separate the serum from fibrin and cells. RPMI cell culture medium with

stable glutamine, supplemented with 10% fetal bovine serum (FBS) and penicillin/streptomycin (1 U/mL) in a humidified atmosphere with 5% CO_2 was used for the oxidation experiments.

The experiments with red blood cells were carried out according to the procedures established in the literature.[26, 38] The blood samples were immediately centrifuged for 10 min at 3000 rpm and the erythrocytes and plasma separated (buffy coat was removed and discarded). To ensure that the hematocrit was maintained, the erythrocytes were resuspended in an equal volume of PBS (Phosphate Buffered Saline; 1.4×10^{-1} M NaCl, 5.0×10^{-3} M NaH_2PO_4, 1.1×10^{-2} M glucose; pH 7.40). The erythrocytes were washed with PBS, centrifuged three times and incubated at 37 °C with solutions containing Metvan. Aliquots were taken at different time points (60, 120, and 180 min) and centrifuged for 10 min at 3000 rpm to separate the solution from the erythrocytes. The erythrocytes were washed two times with PBS and transferred into quartz tubes; at this point, EPR spectra at 120 K were recorded. Even if the freezing produces erythrocyte lysates, the measured EPR spectra coincide with those of intact red blood cells. The determination of V inside the red blood cells was carried out from the EPR intensity of the parallel M_I = -5/2 and perpendicular M_I = 5/2 resonances. In the extracellular medium the V concentration was determined spectrophotometrically based on the reaction with 4-(2-pyridylazo)-resorcinol (PAR),[39] which forms with V^V in the pH range 4.5-8.0 at 37 °C (under the experimental conditions in which the oxidation of V^{IV} to V^V by atmospheric oxygen is rapid and quantitative) an anionic complex $[V^VO_2(PAR)]^-$, with an absorption maximum at λ_{max} = 542 nm and ε_{max} = 3.6-3.7 × 10^4 L mol^{-1} cm^{-1}.[40] The exact procedure was recently described.[30a, 30b]

The oxidation experiments were carried out as follows. RPMI cell culture medium was incubated at 37 °C with a solution containing Metvan to obtain a final V concentration of 4.54×10^{-4} M. Aliquots were taken at different time (0-5 hours), transferred into quartz tubes, frozen at 120 K and used to record EPR spectra. The intensity of the spectral signals was related to the amount of V^{IV} oxidized to V^V.

2.6. Spectroscopic and analytical measurements

Anisotropic EPR spectra were recorded on frozen solutions (120 K) with an X-band (9.4 GHz) Bruker EMX spectrometer equipped with an HP 53150A microwave frequency counter. The microwave frequency used for EPR measurements was 9.40-9.41 GHz (120 K). When the signal to noise ratio was low due to the low $V^{IV}O^{2+}$ concentration, signal averaging was used.[41] Spectrophotometric measurements were carried out with a Perkin-Elmer Lambda 35 spectrophotometer, and the absorption maximum of $[V^VO_2(PAR)]^-$ was read at λ_{max} = 542 nm.

ESI mass spectra in positive- and negative-ion mode were obtained on a Q Exactive™ Plus Hybrid Quadrupole-Orbitrap™ (Thermo Fisher Scientific) mass spectrometer. The solutions were infused at a flow rate of 5.00 μL/min into the ESI chamber immediately after their preparation in order not to modify the aqueous solution equilibria. The spectra were recorded in the *m/z* range 50-750 at a resolution of 140000 and accumulated for at least 2 min in order to increase the signal-to-noise ratio. The experimental conditions used for the measurements in positive mode were: spray voltage 2300 V, capillary temperature 250 °C, sheat gas 5 (arbitrary units), auxiliary gas 3 (arbitrary units), sweep gas 0 (arbitrary units), probe heater temperature 50 °C. The experimental conditions used for the measurements in negative mode were: spray voltage -1900 V, capillary temperature 250 °C, sheat gas 20 (arbitrary units), auxiliary gas 5 (arbitrary units), sweep gas 0 (arbitrary units), probe heater temperature 14 °C. MS/MS experiments were performed using NCE setting in the range 10-30; ion fragments were detected at a resolution of 17500. ESI mass spectra were analysed by using Thermo Xcalibur 3.0.63 software (Thermo Fisher Scientific).

2.7. DFT calculations

All the calculations presented in this paper were carried out with DFT methods using the software Gaussian 03 (revision C.02),[42] and ORCA.[43]

The geometry of the binary complexes formed by $V^{IV}O^{2+}$ and Me_2phen, and those of the ternary species formed by $V^{IV}O^{2+}$, Me_2phen and MeIm were optimized with the functional B3P86 and the basis set 6-311g. This choice ensures a good degree of accuracy in the prediction of the structures of the first-row transition metal complexes [44] and, in particular, of vanadium compounds.[45] For all the structures, minima were verified through frequency calculations.

For the optimized structures, the ^{51}V hyperfine coupling constants (A) were calculated with Gaussian software using the hybrid functional half-and-half BHandHLYP and the basis set 6-311g(d,p) and with ORCA software using the hybrid functional PBE0 and the basis set VTZ, according to the procedures previously published.[46] The theory background was described in detail in ref. [47]. The percent deviation (PD) of the absolute calculated value, $|A_z|^{calcd}$, from the absolute experimental value, $|A_z|^{exptl}$, was obtained as follows: $100 \times [(|A_z|^{calcd} - |A_z|^{exptl})/|A_z|^{exptl}]$.

3. Results and discussion

3.1. Binary system $V^{IV}O$/Me_2phen

After the dissolution of Metvan in water the dissociation reaction $[VO(Me_2phen)_2(SO_4)] + H_2O \rightarrow [VO(Me_2phen)_2(H_2O)]^{2+} + SO_4^{2-}$ takes place, with the water ligand which replaces the weakly coordinated sulphate anion. To understand which complexes are formed by $V^{IV}O^{2+}$ ion and 4,7-dimethyl-1,10-phenanthroline in aqueous solution, the binary system $V^{IV}O^{2+}$/Me_2phen has been studied as a function of pH through the combined application of potentiometric and spectroscopic methods.

In the literature the value of pK_a reported for Me_2phen is 5.95.[48] The presence of the two methyl substituents with electron releasing effect in position 4 and 7 increases the pK_a by one unit (5.95 [48]) with respect to 1,10-phenanthroline (4.93-4.94 [46f, 48]). In this work, we recalculated the value for Me_2phen and found to be 6.01, in good agreement with the previous results.[48] In the $V^{IV}O^{2+}$/Me_2phen system the titration curves could be fitted assuming the formation of mono-, bis-chelated, mono-hydroxido and a dinuclear hydrolytic complex. As Figure 1 reveals, $[VO(Me_2phen)_2(H_2O)]^{2+}$ dominates in the acidic pH range and then the mono-hydroxido complex $[VO(Me_2phen)_2(OH)]^{+}$ is formed with a pK of 5.29, which suggests the deprotonation of an equatorial water molecule to give a OH^- ion. It is noteworthy that the pK_{VOL_2} of 5.29 is comparable with that of similar ligands such as 1,10-phenanthroline (4.75-5.13 [46f, 49]) and 2,2'-bipyridine (4.89 [46f]), and is significantly lower than picolinate, pyronate and pyridinonate derivatives (for which it is in the range 6.07-10.75 [21i, 50]). $[VO(Me_2phen)_2(OH)]^{+}$ is the major species in solution from pH 6.5 to 8.5 and, in particular, at pH 7.4. It survives in solution up to pH around 9.5-10.0. The distribution curves of the species formed with a molar ratio $V^{IV}O^{2+}$/Me_2phen of 1/5 are shown in Figure S1 of ESI.

Table 1. Stepwise deprotonation constants (pK_a) of the ligands and stability constants (logβ) of the binary and ternary complexes formed by $V^{IV}O^{2+}$ with Me_2phen (HL), MeIm (HB), citric acid (H_3B) and lactic acid (HB) at 25.0 ± 0.1 °C and I = 0.20 mol dm^{-3} (KCl).

	Me_2phen	MeIm	Citric acid	Lactic acid
pK_{a1}	6.01(2)	7.13(1)	2.85(1)	3.62(1)
pK_{a2}			4.24(1)	
pK_{a3}			5.55(1)	
logβ_{VOL}	6.91(1)			
logβ_{VOL_2}	11.74(5)			
log$\beta_{VOL_2H_{-1}}$	6.45(6)			

$\log\beta_{VO_2L_2H_{-2}}$	8.08(5)			
$\log\beta_{VOLBH}$			18.27(1)	
$\log\beta_{VOLB}$		12.32(4)	14.85(2)	10.6(1)
$\log\beta_{VOLBH_{-1}}$		6.92(9)	9.07(3)	
$\log\beta_{VOL_2B}$		17.03(10)		

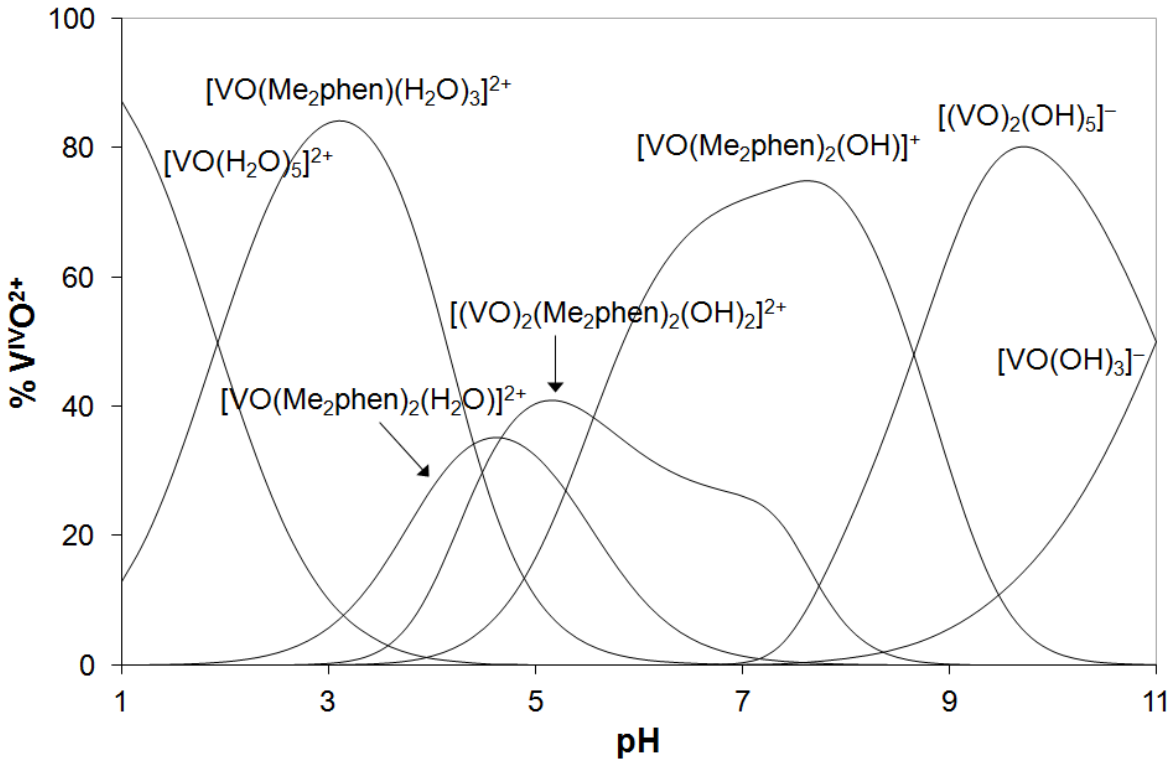

Figure 1. Concentration distribution curves of the species formed in the system $V^{IV}O^{2+}$/Me_2phen with a molar ratio of 1/2 and V concentration of 1.0×10^{-3} M.

EPR spectra as a function of pH (recorded with the same $V^{IV}O^{2+}$ concentration and ligand to metal ratio as shown in Figure 1, i.e. 2/1) are reported in Figure 2. The spectra obtained with L/V^{IV}O ratio of 5/1 are presented in Figure S2 of ESI. The results confirm those obtained with the potentiometric studies: the mono-chelated species $[VO(Me_2phen)(H_2O)_3]^{2+}$ exists in aqueous solution between pH 2.0 and 4.5 in its two isomeric forms, with the ligand assuming an (equatorial-equatorial) and (equatorial-axial) arrangement (a and b in Scheme 2). The two species exist in the pH range 2-4 in comparable amounts (**I** and **II** in Figure 2).

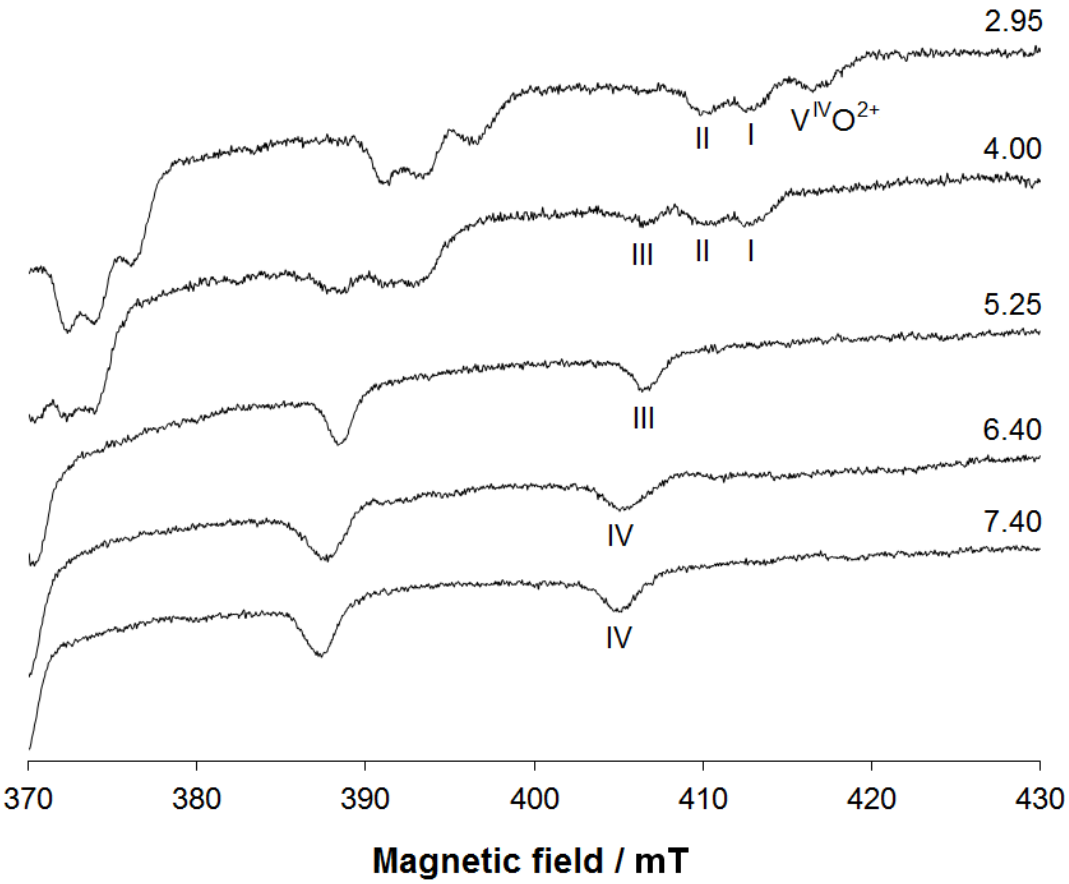

Figure 2. High field region of the X-band anisotropic EPR spectra recorded at 120 K as a function of pH in the system $V^{IV}O^{2+}$/Me_2phen with a molar ratio of 1/2 and V concentration of 1.0×10^{-3} M. The M_I = 7/2 resonance of $[VO(H_2O)_5]^{2+}$ is indicated with $\mathbf{V^{IV}O^{2+}}$, of $[VO(Me_2phen)(H_2O)_3]^{2+}$ (equatorial-equatorial coordination) with **I**, of $[VO(Me_2phen)(H_2O)_3]^{2+}$ (equatorial-axial coordination) with **II**, of *cis*-$[VO(Me_2phen)_2(H_2O)]^{2+}$ with **III** and of *cis*-$[VO(Me_2phen)_2(OH)]^{+}$ with **IV**.

Table 2. Experimental g_z and A_z values of the $V^{IV}O$ species formed in the binary systems $V^{IV}O^{2+}$/Me_2phen and $V^{IV}O^{2+}$/phen.

Ligand	Complex	g_z	A_z / 10^{-4} cm^{-1}	Donors [a]
Me_2phen	$[VO(Me_2phen)(H_2O)_3]^{2+}$	1.941	172.1	2 N_{eq}, 2 H_2O_{eq}, H_2O_{ax}
	$[VO(Me_2phen)(H_2O)_3]^{2+}$	1.948	169.5	N_{eq}, N_{ax}, 3 H_2O_{eq}
	cis-$[VO(Me_2phen)_2(H_2O)]^{2+}$	1.951	162.3	3 N_{eq}, N_{ax}, H_2O_{eq}
	cis-$[VO(Me_2phen)_2(OH)]^{+}$	1.952	158.5	3 N_{eq}, N_{ax}, OH^-_{eq}
phen [b]	$[VO(phen)(H_2O)_3]^{2+}$	1.942	173.1	2 N_{eq}, 2 H_2O_{eq}, H_2O_{ax}
	$[VO(phen)(H_2O)_3]^{2+}$	1.946	170.0	N_{eq}, N_{ax}, 3 H_2O_{eq}

cis-$[VO(phen)_2(H_2O)]^{2+}$	1.949	162.7	3 N_{eq}, N_{ax}, H_2O_{eq}
cis-$[VO(phen)_2(OH)]^{+}$	1.950	158.9	3 N_{eq}, N_{ax}, OH^-_{eq}

[a] The subscripts eq and ax indicate the donors coordinated in the equatorial and axial position of the coordination sphere of $V^{IV}O^{2+}$ ion. [b] Values taken from ref. 46f.

Similarly to what was reported for 1,10-phenanthroline,[46f] the value of A_z for mono-chelated species $[VO(Me_2phen)(H_2O)_3]^{2+}$ with (equatorial-equatorial) coordination (**I** in Figure 2 and a in Scheme 2), 172.1 × 10^{-4} cm^{-1}, is larger than that of the isomer with (equatorial-axial) coordination (**II** in Figure 2 and b in Scheme 2), 169.5 × 10^{-4} cm^{-1} (Table 2). This apparent anomaly, related to the fact that the 'additivity relationship' suggests that an equatorial donor should give a lower contribution to A_z than an axial donor,[51, 52, 53] has been explained carrying out DFT calculations and can be rationalized considering that a pyridine ring perpendicular to V=O bond (equatorial-equatorial coordination) gives an A_z value significantly larger than a ring parallel to V=O (equatorial-axial coordination).[54]

In the spectrum recorded at pH 4.00 another species is revealed (**III** in Figure 2 and c in Scheme 2); on the basis of pH-potentiometric and spectroscopic data, to this complex with stoichiometry $[VO(Me_2phen)_2(H_2O)]^{2+}$ a *cis*-octahedral structure is assigned. This species is converted at pH values higher than 5 (note the enlargement to the downfield of the resonances of **III**) to the corresponding mono-hydroxido complex *cis*-$[VO(Me_2phen)_2(OH)]^{+}$ (**IV** in Figure 2 and d in Scheme 2) upon the deprotonation of the water ligand coordinated in the equatorial position.

The comparison between the systems $V^{IV}O^{2+}$/Me_2phen and $V^{IV}O^{2+}$/phen indicates that the hyperfine coupling constants of the complexes formed by dimethyl derivative are slightly smaller than those of the species of 1,10-phenanthroline (Table 2). This can be put into relationship with the higher basicity of Me_2phen (about one log unit, see above), for which the electron releasing effect of the methyl groups increases the electronic density at the N donors.

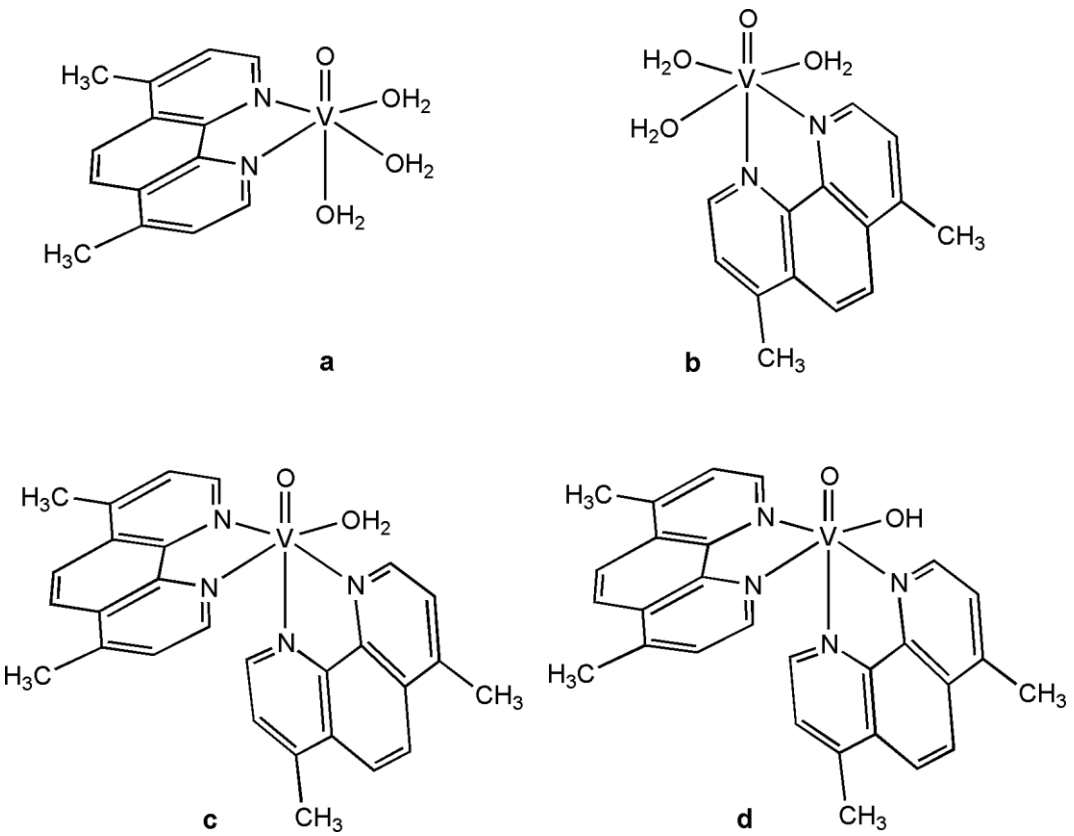

Scheme 2. Structure of the species existing in aqueous solution at different pH values in the system $V^{IV}O^{2+}$/Me_2phen: a) $[VO(Me_2phen)(H_2O)_3]^{2+}$ (equatorial-equatorial coordination); b) $[VO(Me_2phen)(H_2O)_3]^{2+}$ (equatorial-axial coordination); c) *cis*-$[VO(Me_2phen)_2(H_2O)]^{2+}$ and d) *cis*-$[VO(Me_2phen)_2(OH)]^{+}$.

ESI-MS spectrum was recorded at spontaneous pH (4.80) in ultrapure LC-MS water with a V final concentration of 1.0×10^{-5} M (Figure S3 of ESI). All the fragments revealed were listed in Table 3. The mass spectrum shows peaks at m/z = 209.11 attributed to the protonated form of the ligand $[Me_2phen+H]^{+}$, at m/z = 241.57 attributed to $[V^{IV}O(Me_2phen)_2]^{2+}$ without the water molecule, at m/z = 292.04 attributed to the mono-chelated complex $[V^{IV}O(Me_2phen)(OH)]^{+}$, and at m/z = 499.13 attributed to $[V^{V}O_2(Me_2phen)_2]^{+}$. This confirms the presence in solution, under these experimental conditions, of the mono- and bis-chelated species. However, the examination of the spectrum suggests two important observations: i) as pointed out in the literature, a solvent molecule with monodentate coordination can be removed from the metal during the ionization process;[55] the detection of $[V^{V}O_2(Me_2phen)_2]^{+}$ can be related to the formation of $[V^{IV}O(Me_2phen)_2(H_2O)]^{2+}$ in the $V^{IV}O^{2+}$/Me_2phen system and is due to two (partial) oxidation processes, in solution and in-source during the recording of the spectrum.[56] The oxidation is probably favored by the structure of *cis*-

$V^{IV}O(H_2O)^{2+}$ moiety which gives the *cis*-$V^{V}O^{2+}$ ion without any structural rearrangement (Scheme 3a).

Table 3. Species identified from the ESI-MS studies and MS/MS fragmentation products.

Species	Composition	$(m/z)^{exptl\ a}$	$(m/z)^{calcd\ a}$	Dev. (ppm) [b]
$[Me_2phen+H]^+$	$C_{14}H_{13}N_2$	209.10736	209.10732	0.19
$[V^{IV}O(Me_2phen)_2]^{2+}$	$C_{28}H_{24}N_4OV$	241.56891	241.56894	-0.12
$[V^{IV}O(Me_2phen)(OH)]^+$	$C_{14}H_{13}N_2O_2V$	292.04111	292.04112	-0.03
$[V^{V}O_2(Me_2phen)_2]^+$	$C_{28}H_{24}N_4O_2V$	499.13385	499.13334	1.02
$[V^{V}O_2(Me_2phen)]^+$ [c]	$C_{14}H_{12}N_2O_2V$	291.03330	291.03329	0.03
$[V^{V}O_2(Me_2phen)(H_2O)]^+$ [c]	$C_{14}H_{14}N_2O_3V$	309.04405	309.04386	0.61
$[Hcitr]^{2-}$	$C_6H_6O_7$	95.00492	95.00622	-13.68
$[H_2citr]^-$	$C_6H_7O_7$	191.01896	191.01973	-4.03
$[V^{IV}O(Me_2phen)(citr)]^-$	$C_{20}H_{17}N_2O_8V$	464.04305	464.04300	0.11
$[V^{IV}O(citr)]^-$ [d]	$C_6H_5O_8V$	255.94291	255.94295	-0.16
$[V^{IV}O(Me_2phen)(citr)+2H]^+$	$C_{20}H_{19}N_2O_8V$	466.05736	466.05756	-0.43
$[V^{V}O_2(Me_2phen)(lact)+H]^+$	$C_{17}H_{18}N_2O_5V$	381.06490	381.06499	-0.24

[a] The experimental ($(m/z)^{exptl}$) and calculated ($(m/z)^{calcd}$) m/z values refer to the peak representative of the monoisotopic mass. [b] Deviation from the experimental value in ppm, calculated as $10^6 \times [(m/z)^{calcd} - (m/z)^{exptl}]/(m/z)^{exptl}$. [c] Originated in the ESI-MS/MS spectrum from $[V^{V}O_2(Me_2phen)_2]^+$. [d] Originated in the ESI-MS/MS spectrum from $[V^{IV}O(Me_2phen)(citr)]^-$.

Calculated and experimental isotopic pattern for the $V^{IV}O$ complexes are reported in Figures S4-S6 of ESI. In particular, the peaks due to the natural abundance of ^{13}C (separated by m/z ~ 1.00 when the charge of the fragment is +1, and by m/z ~ 0.50 when it is +2) allowed us to confirm the attribution proposed above. A further demonstration can be obtained by ESI-MS/MS experiments: for example, the ESI-MS/MS spectrum recorded in the range m/z = 499.5 ± 1.0 (where the peak of $[V^{V}O_2(Me_2phen)_2]^+$ falls) shows the peaks at 291.03 and 309.04, attributed to the fragments $[V^{V}O_2(Me_2phen)]^+$ and $[V^{V}O_2(Me_2phen)(H_2O)]^+$ generated upon the loss of one ligand molecule (Figure S7).

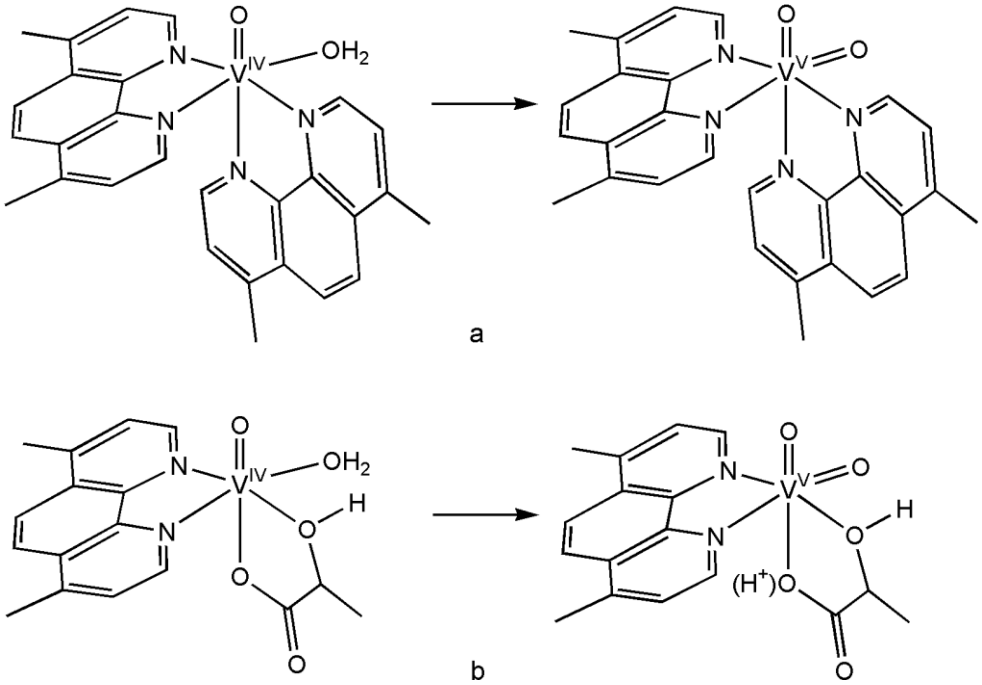

Scheme 3. Oxidation processes of *cis*-$[VO(Me_2phen)_2(H_2O)]^{2+}$ to give *cis*-$[V^{V}O_2(Me_2phen)_2]^{+}$ (a) and *cis*-$[VO(Me_2phen)(lact)(H_2O)]^{+}$ to give [*cis*-$V^{V}O_2(Me_2phen)(lact)+H]^{+}$ (b).

The structures of the most relevant species in the pH range 5-9, *cis*-$[VO(Me_2phen)_2(H_2O)]^{2+}$ and *cis*-$[VO(Me_2phen)_2(OH)]^{+}$, have been optimized with software Gaussian 03 [42] through DFT methods, which allow one to obtain good predictions of the geometry of complexes formed by transition metals,[44, 57] and particularly by $V^{IV}O^{2+}$ ion.[21e] These structures are shown in Figure 3 (a and b).

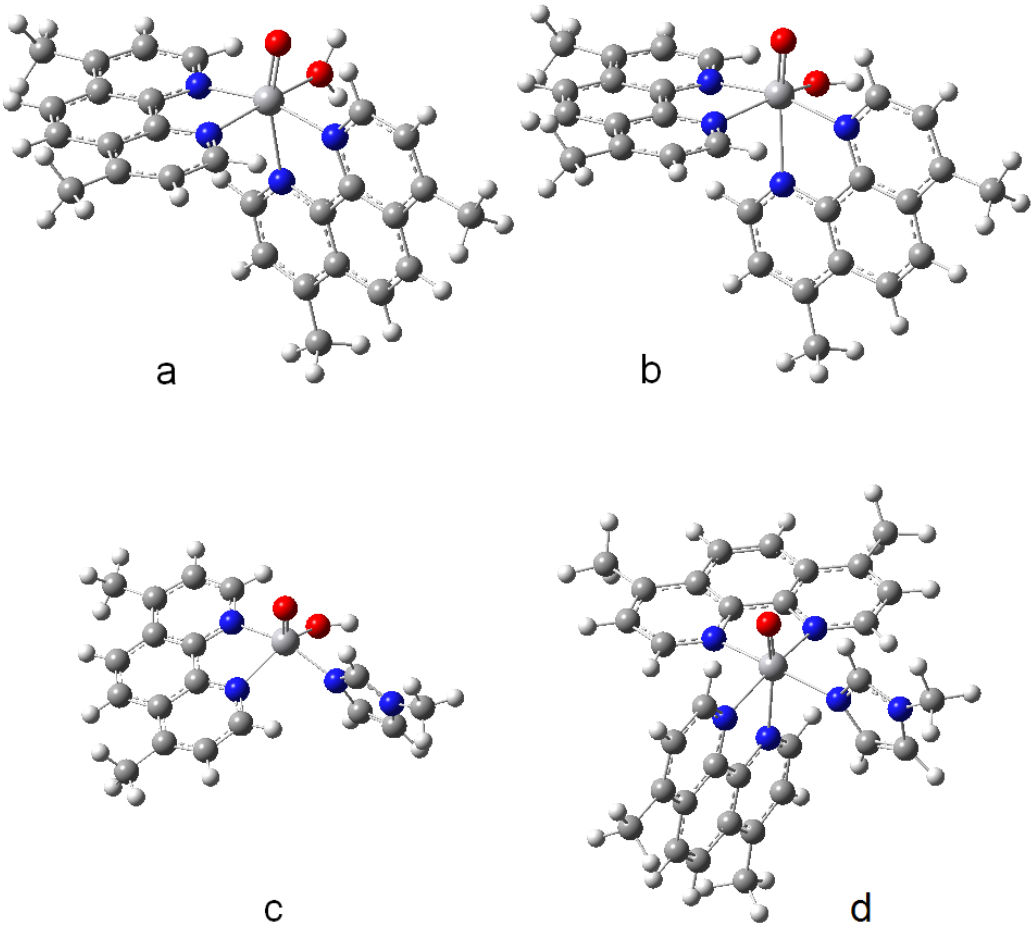

Figure 3. Structure of the complexes *cis*-$[VO(Me_2phen)_2(H_2O)]^{2+}$ (a), *cis*-$[VO(Me_2phen)_2(OH)]^{+}$ (b), $[VO(Me_2phen)(MeIm)(OH)]^{+}$ (c) and *cis*-$[VO(Me_2phen)_2(MeIm)]^{2+}$ (d), optimized by DFT methods at level of theory B3P86/6-311g.

DFT methods also allowed us to predict the values of ^{51}V A_z constants for the major $V^{IV}O$ complexes.[58] A good agreement with the experimental data can be obtained with Gaussian (second-order contribution to A_z related to the spin-orbit effect not included in the calculations) and ORCA (second-order contribution to A_z included in the calculations).[47b, 54] A_z for *cis*-$[VO(Me_2phen)_2(H_2O)]^{2+}$ and *cis*-$[VO(Me_2phen)_2(OH)]^{+}$ are reported in Table 4. It can be noticed that the results are in good agreement with the experiment: although both Gaussian and ORCA underestimate $|A_z|$, the first software works slightly better than the second one.[47b] As experimentally observed, the value of $|A_z|$ decreases significantly from *cis*-$[VO(Me_2phen)_2(H_2O)]^{2+}$ to *cis*-$[VO(Me_2phen)_2(OH)]^{+}$.

Table 4. Experimental and calculated values of ^{51}V A_z for *cis*-$[VO(Me_2phen)_2(H_2O)]^{2+}$, *cis*-$[VO(Me_2phen)_2(OH)]^{+}$, $[VO(Me_2phen)(MeIm)(H_2O)]^{2+}$, $[VO(Me_2phen)(MeIm)(OH)]^{+}$ and *cis*-$[VO(Me_2phen)_2(MeIm)]^{2+}$.[a]

	Exptl.	Calcd. (Gaussian)		Calcd. (ORCA)	
Complex	A_z	A_z	PD [b]	A_z	PD [b]
cis-$[VO(Me_2phen)_2(H_2O)]^{2+}$	-162.3	-160.7	-1.0	-157.9	-2.7
cis-$[VO(Me_2phen)_2(OH)]^{+}$	-158.7	-153.5	-3.3	-148.4	-6.5
$[VO(Me_2phen)(MeIm)(H_2O)]^{2+}$	-168.9	-167.5	-0.8	164.8	-2.4
$[VO(Me_2phen)(MeIm)(OH)]^{+}$	-162.0	-154.7	-4.5	-151.8	-6.3
cis-$[VO(Me_2phen)_2(MeIm)]^{2+}$	-160.3	-152.3	-5.0	-149.4	-6.8
Mean percent deviation (MPD)	–	–	-2.9	–	-4.9

[a] Values reported in 10^{-4} cm^{-1}. [b] Percent deviation of the absolute calculated value, $|A_z|^{calcd}$, from the absolute experimental value, $|A_z|^{exptl}$, obtained as follows: $100 \times [(|A_z|^{calcd} - |A_z|^{exptl})/|A_z|^{exptl}]$.

3.2. Ternary systems $V^{IV}O$/Me_2phen/citrate and $V^{IV}O$/Me_2phen/lactate

It has been demonstrated by some of us that, among the l.m.m. bioligands of the blood plasma, citrate and lactate have the greatest affinity to $V^{IV}O^{2+}$ ion.[21a] Their fully protonated form will be indicated with H_3citr (three protons titratable in aqueous solution) and Hlact (one proton titratable in aqueous solution). Concerning the other potential ligands, they are present in too small concentration (oxalate) or they have low affinity for $V^{IV}O^{2+}$ ion (amino acids, phosphates, sulphate, carbonate). Therefore, in this work, to understand the speciation of Metvan under the physiological conditions, the ternary systems $V^{IV}O^{2+}$/Me_2phen/H_3citr and $V^{IV}O^{2+}$/Me_2phen/Hlact have been examined.

Potentiometry indicates that, with citrate, three mixed species with composition $[VO(Me_2phen)(citrH)]$, $[VO(Me_2phen)(citr)]^{-}$ and $[VO(Me_2phen)(citrH_{-1})]^{2-}$ exist in solution (see Table 1). The distribution curves of the species formed as a function of pH with a molar ratio $V^{IV}O^{2+}$/Me_2phen/H_3citr of 1/2/2 and V concentration of 1.0×10^{-3} M are shown in Figure 4. Since Me_2phen can coordinate the $V^{IV}O^{2+}$ ion exclusively with the donor set (N, N), it is citrate, in the different protonated states, which changes its coordination mode in the three ternary complexes. In particular, this should be (COO^{-}, OH, COO^{-ax}) in the first two species (with the non-coordinating carboxylic group protonated in $[VO(Me_2phen)(citrH)]$ and deprotonated in $[VO(Me_2phen)(citr)]^{-}$) and (COO^{-}, O^{-}, COO^{-ax}) in the third one (Scheme 4, a-c). These species exist in the pH range 2-4,

3-6 and 6-10, respectively. From an examination of Figure 4, it emerges that the most important species at pH 7.4 is $[VO(Me_2phen)(citrH_{-1})]^{2-}$.

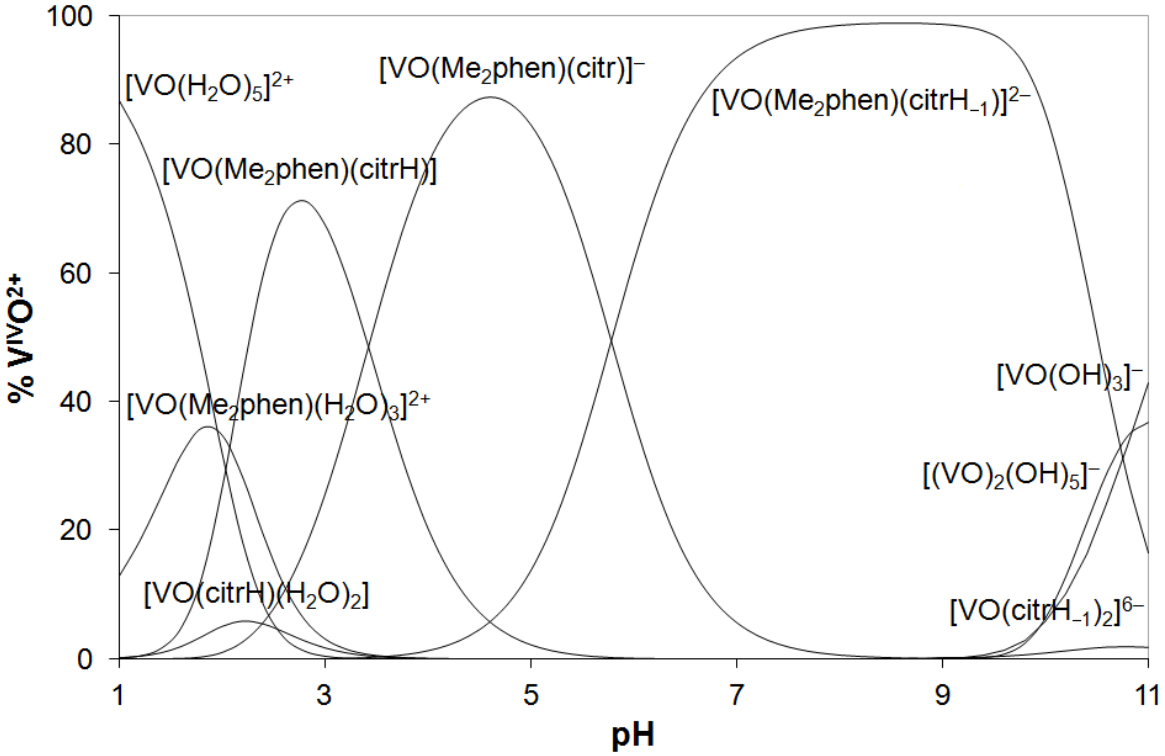

Figure 4. Concentration distribution curves of the species formed in the system $V^{IV}O^{2+}$/Me_2phen/H_3citr with a molar ratio of 1/2/2 and V concentration of 1.0×10^{-3} M.

The anisotropic EPR spectrum allowed us to confirm the existence of $[VO(Me_2phen)(citrH)]$, $[VO(Me_2phen)(citr)]^-$ and $[VO(Me_2phen)(citrH_{-1})]^{2-}$ in solution (Figure S8 of ESI). $[VO(Me_2phen)(citrH)]$ and $[VO(Me_2phen)(citr)]^-$ are characterized by identical values of g_z and A_z (g_z =1.950 and A_z = 165.1 × 10^{-4} cm^{-1}) because the equatorial coordination is the same ((N, N); (COO^-, OH, COO^{-ax})), whereas $[VO(Me_2phen)(citrH_{-1})]^{2-}$ with ((N, N); (COO^-, O^-, COO^{-ax}) coordination has g_z = 1.952 and A_z = 158.1 × 10^{-4} cm^{-1} (Table 5). The structure of $[VO(Me_2phen)(citrH_{-1})]^{2-}$ is represented in Scheme 4c and indicates that at pH 7.4 citrate replaces one of the two Me_2phen ligands in $[VO(Me_2phen)_2(OH)]^+$, behaving as a tridentate ligand, with the contemporaneous binding of one carboxylate and the alkoxide group in the equatorial plane and of another carboxylate in the axial position.

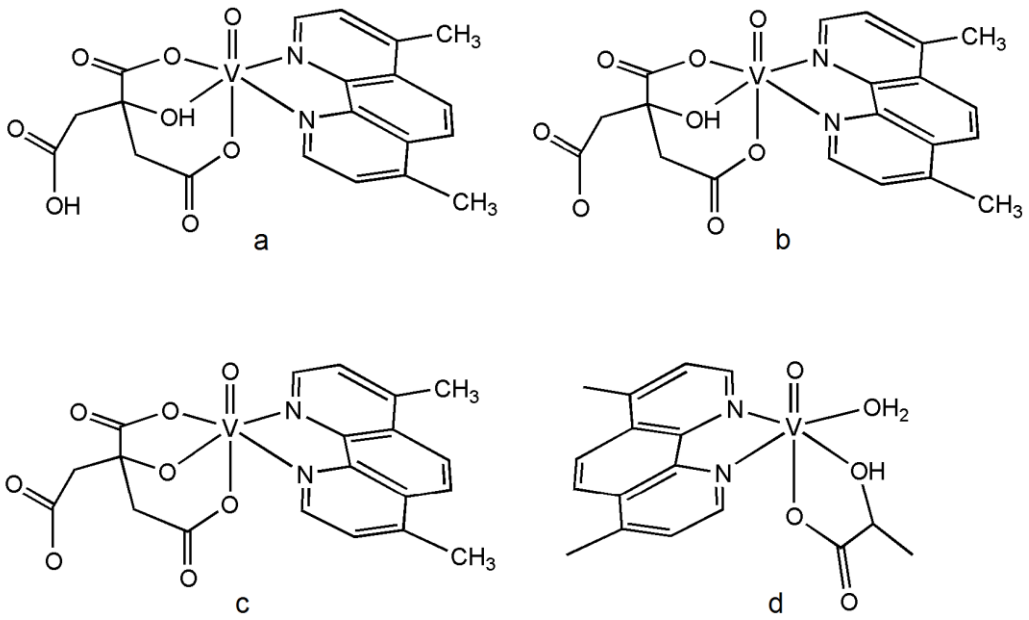

Scheme 4. Structure of the mixed species [VO(Me$_2$phen)(citrH)] (a), [VO(Me$_2$phen)(citr)]$^-$ (b), [VO(Me$_2$phen)(citrH$_{-1}$)]$^{2-}$ (c) and [VO(Me$_2$phen)(lact)]$^+$ (d).

Negative ESI-MS spectrum was recorded in the system $V^{IV}O^{2+}$/Me$_2$phen/H$_3$citr at pH 4.90 in ultrapure LC-MS water and is shown in Figure S9 of ESI. The peaks at m/z = 95.00 and 191.02 can be assigned to the bianionic and monoanionic forms of citrate, respectively, whereas that at m/z = 255.94 to [V^{IV}O(citr)]$^-$ with citrate in its triply deprotonated form (Table 3).

One important peak appears at m/z = 464.04 and is attributed to the mixed species [V^{IV}O(Me$_2$phen)(citr)]$^-$ (Table 3). Calculated and experimental isotopic pattern for the peak of [V^{IV}O(Me$_2$phen)(citr)]$^-$ are reported in Figure S10 of ESI. Interestingly, the fragmentation profile of the negative ESI-MS/MS spectrum recorded in the range m/z = 464.0 ± 1.0 (corresponding to [V^{IV}O(Me$_2$phen)(citr)]$^-$) shows the species [V^{IV}O(citr)]$^-$ (m/z = 255.94) obtained from [V^{IV}O(Me$_2$phen)(citr)]$^-$ upon the loss of one Me$_2$phen ligand (Figure S11).

Positive ESI-MS spectrum of the system $V^{IV}O^{2+}$/Me$_2$phen/H$_3$citr 1/2/2 at pH 4.80 is similar to that recorded in the system $V^{IV}O^{2+}$/Me$_2$phen with the peaks of the binary species at m/z 241.57 and 499.13 (Table 3), because the positive mode favors the complexes between $V^{IV}O^{2+}$ and Me$_2$phen, positively charged. The peak at m/z = 466.06 is, instead, attributable to [V^{IV}O(Me$_2$phen)(citr)+2H]$^+$ (Table 3); the calculated isotopic pattern and the comparison with the experimental peak is shown in Figure S12 of ESI.

In the ternary system $V^{IV}O^{2+}$/Me_2phen/Hlact the pH-potentiometry indicates the formation of a only one mixed ligand species $[VO(Me_2phen)(lact)]^+$ (Scheme 4, d), which exists in the pH range 2-6, with the coordination of lactate through the donor set (COO^-, OH). The distribution curves of the species formed in the mixed system as a function of pH are shown in Figure 5; from these curves, it can be observed that at pH 7.4 the major species is $[VO(Me_2phen)_2(OH)]^+$ (74.0% for the potentiometry if the ratio $V^{IV}O^{2+}$/Me_2phen/Hlact is 1/2/4) and the minor ones are $[(VO)_2(Me_2phen)_2(OH)_2]^{2+}$ and $[VO(lactH_{-1})_2]^{2-}$ (12.4% and 11.1%, respectively).

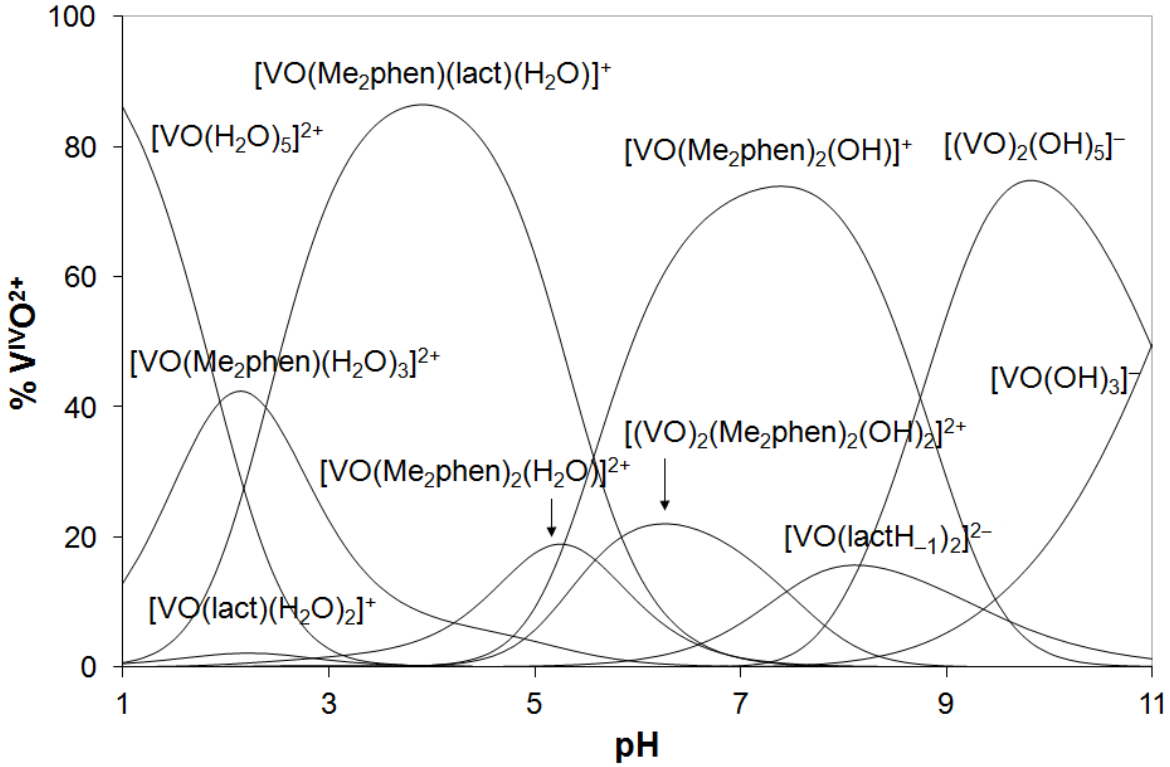

Figure 5. Concentration distribution curves of the species formed in the system $V^{IV}O^{2+}$/Me_2phen/Hlact with a molar ratio of 1/2/4 and V concentration of 1.0×10^{-3} M.

The EPR spectra recorded as a function of pH are reported in Figure S13 of ESI. The signals of $[VO(Me_2phen)(lact)(H_2O)]^+$ appear from pH 4 to 6, as predicted by pH-potentiometry measurements. The values of g_z and A_z are 1.946 and 166.3×10^{-4} cm^{-1} (Table 5). The slight increase of value of A_z with respect to the analogous complex with citrate can be rationalized through the 'additivity relationship',[51, 52, 53] advancing the hypothesis that a water instead of a carboxylate donor occupies the equatorial position of $V^{IV}O^{2+}$ ion (cfr. structures b and d in Scheme 4). Such a structure with an equatorial water molecule was already proposed for ternary complexes

formed by $V^{IV}O^{2+}$, lactate and a bidentate ligands L such as maltolate and picolinate derivatives.[21g, 50c]

The positive ESI-MS spectrum of the system $V^{IV}O^{2+}$/Me_2phen/Hlact, recorded in ultrapure water with a molar ratio of 1/2/4 and pH 3.80, shows a peak at m/z = 381.07 which is attributed to the ternary complex $[V^{V}O_2(Me_2phen)(lact)+H]^+$. Experimental and calculated isotopic pattern for this peak are reported in Figure S14 of ESI. It is noteworthy the coincidence of the two expected peaks derived from the presence of ^{13}C isotope at the third decimal figure. The detection of V^V species $[V^{V}O_2(Me_2phen)(lact)+H]^+$ can be explained in terms of the in-source oxidation of $[V^{IV}O(Me_2phen)(lact)(H_2O)]^+$ (Scheme 3b), confirming that the structure of the mixed species $V^{IV}O^{2+}$–Me_2phen–lact has an equatorial water.

Therefore, the spectroscopic, spectrometric and potentiometric measurements suggest that, in contrast to the system containing citrate, under physiological pH the formation of mixed species with lactate can be ruled out. The result can be explained with the fact that at pH 7.4 the bidentate (O, O) lactate ligand is less effective than citrate (which acts as a tridentate ligand) and is not able to replace Me_2phen in the coordination sphere of oxidovanadium(IV) ion.

Table 5. EPR parameters of the mixed complexes formed at pH 7.4 in the ternary systems with Me_2phen and citrate, lactate, MeIm, apo-hTf, holo-hTf, HSA, and Hb.

Mixed complex	$V^{IV}O$/Me_2phen/ bioligand	g_z	A_z [a]	Donors [b]
cis-$[VO(Me_2phen)_2(OH)]^+$	1/2/0	1.953	158.7	(N, N); (N, N^{ax}); OH^-
$[VO(Me_2phen)(citrH)]$	1/2/2	1.950	165.1	(N, N); (COO^-, OH, COO^{-ax})
$[VO(Me_2phen)(citr)]^-$	1/2/2	1.950	165.1	(N, N); (COO^-, OH, COO^{-ax})
$[VO(Me_2phen)(citrH_{-1})]^{2-}$	1/2/2	1.952	158.1	(N, N); (COO^-, O^-, COO^{-ax})
$[VO(Me_2phen)(lact)(H_2O)]^+$	1/2/4	1.946	166.3	(N, N); (OH, COO^{-ax}); H_2O
$[VO(Me_2phen)(MeIm)(H_2O)]^{2+}$	1/1/4	1.951	168.9	(N, N); N_{imid}; H_2O
$[VO(Me_2phen)(MeIm)(OH)]^+$	1/1/4	1.953	162.0	(N, N); N_{imid}; OH^-
cis-$[VO(Me_2phen)_2(MeIm)]^{2+}$	1/5/4	1.952	160.8	(N, N); (N, N^{ax}); N_{imid}
VO–Me_2phen–apo-hTf	2/4/1	1.953	158.5	[(N, N); N_{His}; OH^-] + [(N, N); (N, N^{ax}); N_{His}] + [(N, N); X; Y]
VO–Me_2phen–apo-hTf	2/10/1	1.952	158.7	

VO–Me_2phen–holo-hTf	2/4/1	1.954	158.8	[(N, N); N_{His}; OH^-] + [(N, N); (N, N^{ax}); N_{His}] + [(N, N); X; Y]
VO–Me_2phen–holo-hTf	2/10/1	1.952	159.0	
VO–Me_2phen–HSA	4/8/1	1.953	158.5	[(N, N); N_{His}; OH^-] + [(N, N); (N, N^{ax}); N_{His}] + [(N, N); X; Y]
VO–Me_2phen–HSA	4/20/1	1.952	159.6	
VO–Me_2phen–Hb	2/4/1	1.953	158.7	[(N, N); N_{His}; OH^-] + [(N, N); (N, N^{ax}); N_{His}] + [(N, N); X; Y]
VO–Me_2phen–Hb	2/10/1	1.953	160.3	

[a] Absolute values reported in 10^{-4} cm^{-1}. [b] X and Y indicate two generic residues.

3.3. Ternary systems $V^{IV}O$/Me_2phen/MeIm, $V^{IV}O$/Me_2phen/hTf and $V^{IV}O$/Me_2phen/HSA

In this study the interaction of Metvan with the most important proteins of the blood plasma such as transferrin (hTf) and albumin (HSA) was also examined.[21b, 21c] We have shown that 1-methylimidazole (MeIm) is a good model for the monodentate coordination of a His-N of a protein, and that the side-chain of surface and accessible histidines can be compared, both as structure and basicity, to a substituted imidazole.[21b, 21c, 21e] This is confirmed by the fact that the thermodynamic stability constants of the ternary complexes formed by 1-methylimidazole measured by potentiometry are very close to those of the ternary species formed by proteins measured by EPR spectroscopy.[21c, 21e 21g] For example for 1,2-dimethyl-3-hydroxy-4(1*H*)-pyridinone (Hdhp) – which forms the potent insulin-enhancing compound $[VO(dhp)_2]$ [59] –, logβ for $[VO(dhp)_2(MeIm)]$ is 25.4,[21c] for $VO(dhp)_2$(apo-hTf) is 25.5,[21c] for $VO(dhp)_2$(HSA) is 25.9,[21c] and for $VO(dhp)_2$(IgG) is 25.6.[21d]

The ternary system $V^{IV}O^{2+}$/Me_2phen/MeIm was studied through the combined application of EPR spectroscopy, ESI-MS spectrometry and pH-potentiometry. The formation of mixed species depends on pH and metal ion to ligand ratio. An equimolar ratio $Me_2phen/V^{IV}O^{2+}$ favors $[VO(Me_2phen)(MeIm)(H_2O)]$ (Scheme 5, a) at acidic pH and $[VO(Me_2phen)(MeIm)(OH)]^+$ (Scheme 5, b) at neutral pH, whereas at higher ratios $Me_2phen/V^{IV}O$ the formation of *cis*-$[VO(Me_2phen)_2(MeIm)]^{2+}$ is expected (Scheme 5, c). The p*K* of deprotonation of the water molecule in $[VO(Me_2phen)(MeIm)(H_2O)]$ is 5.40 (Table 1). At physiological pH, the major species are $[VO(Me_2phen)(MeIm)(OH)]^+$ and $[VO(Me_2phen)_2(MeIm)]^{2+}$: if $V^{IV}O^{2+}$ concentration is 1.0 ×

10^{-3} M and MeIm is 4.0×10^{-3} M, their percentages in solution are 94.6 and 0.9% ($Me_2phen/V^{IV}O$ = 1), 68.3 and 23.2% ($Me_2phen/V^{IV}O$ = 2), and 31.5 and 51.5% ($Me_2phen/V^{IV}O$ = 5). All the three mixed species were also characterized by EPR spectroscopy (Tables 4 and 5) and DFT calculations (Figure 3 and Table 4); in particular, the value of A_z for *cis*-$[VO(Me_2phen)_2(MeIm)]^{2+}$ (Scheme 5c) is slightly smaller than that of $[VO(Me_2phen)(MeIm)(OH)]^{+}$ (Table 4). No peaks attributable to these mixed complexes can be revealed in the ESI-MS spectra but this could be due to the removal from the first coordination sphere of the metal ion during the ionization process.[55]

The concentration distribution curves of the species formed in the system $V^{IV}O^{2+}/Me_2phen/MeIm$ with a molar ratio of 1/2/4 are represented in Figure 6, whereas those at molar ratio of 1/5/4 in Figure S15 of ESI. It can be noticed that at pH 7.4 the two major species *cis*-$[VO(Me_2phen)_2(MeIm)]^{2+}$ and $[VO(Me_2phen)(MeIm)(OH)]^{+}$ coexist with a small amount of *cis*-$[VO(Me_2phen)_2(OH)]^{+}$ (23.2, 68.3 and 7.7%, respectively). The replacement of the equatorial hydroxide ion by the imidazole-N was already observed for the bis-chelated $V^{IV}O$ complex of picolinic acid which, around the physiological pH, transforms from *cis*-$[VO(pic)_2(OH)]^{-}$ to *cis*-$[VO(pic)_2(MeIm)]$ in the presence of 1-methylimidazole.[21c]

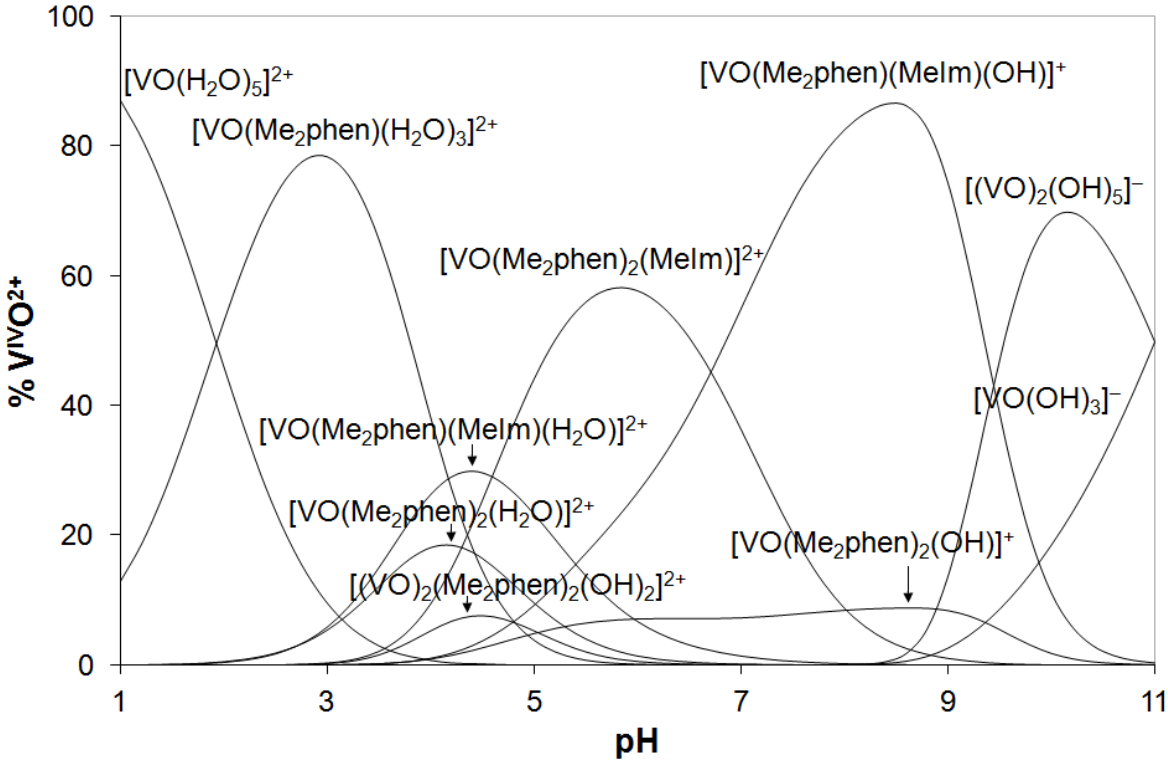

Figure 6. Concentration distribution curves of the species formed in the system $V^{IV}O^{2+}/Me_2phen/MeIm$ with a molar ratio of 1/2/4 and V concentration of 1.0×10^{-3} M.

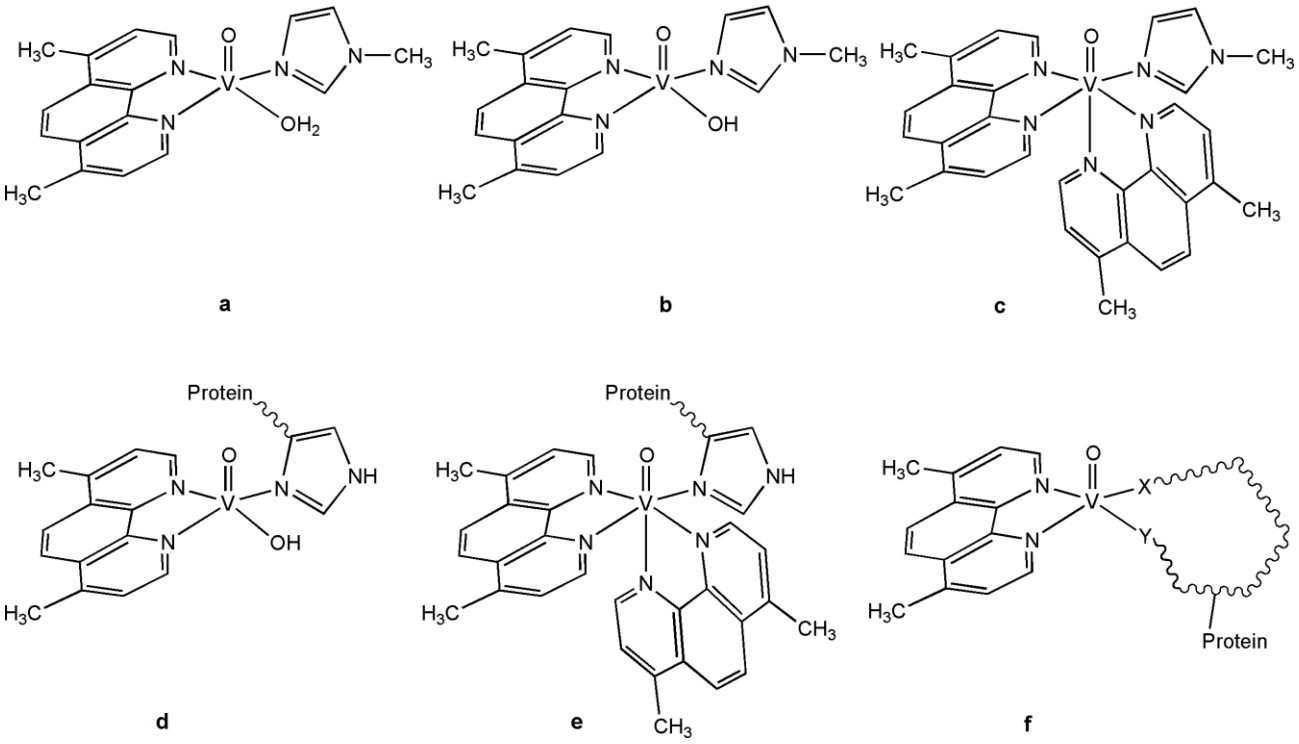

Scheme 5. Structure of the mixed species formed by MeIm and proteins: (a) $[VO(Me_2phen)(MeIm)(H_2O)]^{2+}$; (b) $[VO(Me_2phen)(MeIm)(OH)]^{+}$; c) *cis*-$[VO(Me_2phen)_2(MeIm)]^{2+}$; d) $VO(Me_2phen)(Protein)(OH)$; e) *cis*-$VO(Me_2phen)_2(Protein)$ and g) VO–Me_2phen–Protein, with the Protein interacting with two general residues X and Y. Protein indicates apo-hTf, holo-hTf, HSA or Hb.

EPR spectra recorded at pH 7.4 in the ternary system $V^{IV}O^{2+}$/Me_2phen/MeIm are characterized by a composite M_I = 7/2 resonance, which shifts to lower magnetic field by increasing the ratio $Me_2phen/V^{IV}O$ (cfr. traces a and e in Figure 7). As suggested by potentiometry, this can be explained with the increase of the relative amount of *cis*-$[VO(Me_2phen)_2(MeIm)]^{2+}$ (smaller A_z) with respect to $[VO(Me_2phen)(MeIm)(OH)]^{+}$ (larger A_z). The variation of A_z from $[VO(Me_2phen)(MeIm)(OH)]^{+}$ to *cis*-$[VO(Me_2phen)_2(MeIm)]^{2+}$ is in agreement with the results of DFT calculations (Tables 4 and 5).

The EPR spectra recorded at pH 7.4 in the ternary system $V^{IV}O^{2+}$/Me_2phen/HSA are shown in traces c and d of Figure 7. They are characterized by one set of resonances – indicating that only one species exists in aqueous solution – and by g_z 1.953 and A_z 158.5 × 10^{-4} cm^{-1} when $Me_2phen/V^{IV}O$ = 2 and g_z 1.952 and A_z 159.6 × 10^{-4} cm^{-1} when $Me_2phen/V^{IV}O$ = 5 (Table 5). The spin Hamiltonian parameters are comparable to those of the mixed species

[VO(Me$_2$phen)(MeIm)(OH)]$^+$ and *cis*-[VO(Me$_2$phen)$_2$(MeIm)]$^{2+}$ and, for this reason, the presence in solution of the analogous species of HSA – where the protein equatorially binds $V^{IV}O^{2+}$ ion with a His-N – could be supposed, similarly to what discussed in the literature for other systems [VOL$_2$]/HSA.[21b, 21e, 22b, 22d] The stoichiometry of these species should be indicated with VO(Me$_2$phen)(HSA)(OH) (Scheme 5, d) and *cis*-VO(Me$_2$phen)$_2$(HSA) (Scheme 5, e) or, alternatively, with {VO(Me$_2$phen)(OH)}$_x$(HSA) and {VO(Me$_2$phen)$_2$}$_x$(HSA), where x is the number of accessible His residue which can bind the metal ion. The slight variation of A_z values (see the dotted line in Figure 7 for the comparison of the exact position of the M_I = 7/2 resonance) suggests that each system behaves differently from the other ones and this would be compatible with the presence in aqueous solution of different species under the experimental conditions examined. Such a variation of A_z can be attributed to the differences in the relative amount of VO(Me$_2$phen)(HSA)(OH), *cis*-VO(Me$_2$phen)$_2$(HSA) and *cis*-[VO(Me$_2$phen)$_2$(OH)]$^+$ which causes a shift of the resonances (the relative amount of these three species depends, as discussed above, by the Me$_2$phen/VO^{2+} ratio). Another factor which certainly influences A_z is the "availability" of His side chains for the metal coordination (in fact, the imidazole residues can be more or less exposed on the protein surface and their chemical environment influences the eventual binding to the metal ions). Moreover, the contribution of an imidazole-N to A_z changes as a function of the orientation of the aromatic ring with respect to the V=O bond (A_z(imid-N) = 42.72 + 2.96 × sin(2θ–90), where θ is the dihedral angle defined by the V=O and N–C directions and C is the carbon atom bridging the two nitrogens [52, 60]) and it is plausible that the dihedral angle θ assumes values slightly different in ternary complexes with HSA with respect to the model systems with MeIm as a result of the formation of hydrogen bonds between the imidazole ring and polar groups of neighboring residues. Obviously, the formation of a mixed species with the contemporaneous coordination of two residues of HSA (Scheme 5, g) could not be excluded (see below); this case has been recently reported for Cu^{II} compounds of 2-hydroxy-1-naphthaldehyde benzoyl hydrazone ligand with anti-cancer activity, for which HSA replaces through N donors of Lys-199 and His-242 the monodentate indazole and Br ligands.[61] However, to take into account also this hypothesis, the general formulation VO–Me$_2$phen–HSA (and VO–Me$_2$phen–Protein for the other proteins) will be used from this point forward.

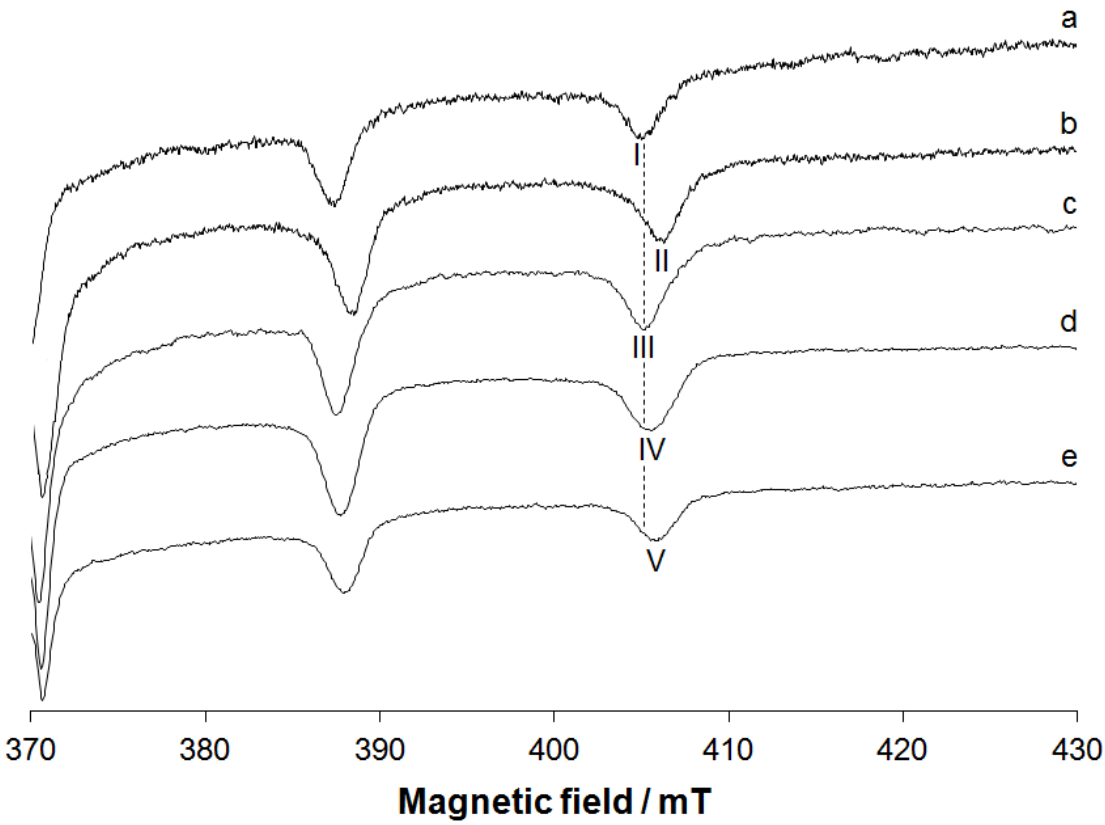

Figure 7. High field region of the X-band anisotropic EPR spectra recorded at 120 K at pH 7.4 in the system containing: a) $V^{IV}O^{2+}$/Me_2phen 1/2 ($V^{IV}O^{2+}$ 1.0 × 10^{-3} M); b) $V^{IV}O^{2+}$/Me_2phen/MeIm 1/2/4 ($V^{IV}O^{2+}$ 1.0 × 10^{-3} M); c) $V^{IV}O^{2+}$/Me_2phen/HSA 4/8/1 ($V^{IV}O^{2+}$ 1.0 × 10^{-3} M); d) $V^{IV}O^{2+}$/Me_2phen/HSA 4/20/1 ($V^{IV}O^{2+}$ 1.0 × 10^{-3} M); e) $V^{IV}O^{2+}$/Me_2phen/MeIm 1/5/4 ($V^{IV}O^{2+}$ 1.0 × 10^{-3} M). The M_I = 7/2 resonance of *cis*-$[VO(Me_2phen)_2(OH)]^+$ is indicated with **I**, of $[VO(Me_2phen)(MeIm)(OH)]^+$ with **II**, of $VO(Me_2phen)(HSA)(OH)$ with **III**, of *cis*-$VO(Me_2phen)_2(HSA)$ with **IV** and of *cis*-$[VO(Me_2phen)_2(MeIm)]^{2+}$ with **V**. The M_I = 7/2 resonance of $VO(Me_2phen)(HSA)(OH)$ is also denoted by the dotted line.

The EPR spectra recorded at pH 7.4 in the ternary systems $V^{IV}O^{2+}$/Me_2phen/apo-hTf and $V^{IV}O^{2+}$/Me_2phen/holo-hTf show only one species (Figure 8, traces c and d); the spin Hamiltonian parameters (Table 5) are very similar to those measured in the system with HSA and depend on the ratio $Me_2phen/V^{IV}O$. Therefore, it can be supposed that apo- and holo-transferrin, similarly to albumin (cfr. traces b-d of Figure 8), replace the OH^- ion or one Me_2phen ligand coordinated in the equatorial plane of $V^{IV}O^{2+}$ in *cis*-$[VO(Me_2phen)_2(OH)]^+$ to form the mixed complexes $VO(Me_2phen)$(apo-hTf)(OH)/$VO(Me_2phen)$(holo-hTf)(OH) (Scheme 5, d) and *cis*-$VO(Me_2phen)_2$(apo-hTf)/*cis*-$VO(Me_2phen)_2$(holo-hTf) (Scheme 5, e). These species are indicated as VO–Me_2phen–apo-hTf and VO–Me_2phen–holo-hTf. Interestingly, their resonances are very

different from those of the binary complexes formed by apo-hTf, (VO)(apo-hTf)/$(VO)_2$(apo-hTf). The coordination mode for $V^{IV}O$–complexes to apo-transferrin was described in terms of Type 1 with a surface His binding to V^{IV}, and Type 2 at the Fe-binding sites; in the first case the interacting residues may be His-14, His-289, His-349, His-350, His-473, His-606 and His-642,[21h] whereas in the second one the donors coordinated to V^{IV} are two among Asp-63, Tyr-95, Tyr-188, His-249.[62] Overall, the results obtained with HSA, apo-hTf and holo-hTf can be interpreted as follows: i) the coincidence of the spectra in the systems $V^{IV}O^{2+}$/Me_2phen/apo-hTf and $V^{IV}O^{2+}$/Me_2phen/holo-hTf suggests that VO–Me_2phen species are not coordinated in the iron sites of transferrin (indeed, for holo-hTf these are occupied by Fe^{3+} ion); ii) the same complex/complexes are formed in the three systems and, for this reason, it is plausible that the proteins bind $V^{IV}O^{2+}$ with only one side chain residue; iii) the contemporaneous binding of two amino acid residues of HSA, apo-hTf and holo-hTf (illustrated in Scheme 5, g) should result in different A_z values (in fact, the possibility that the these donors are the same in the three systems has to be excluded) and must be considered as much less probable.

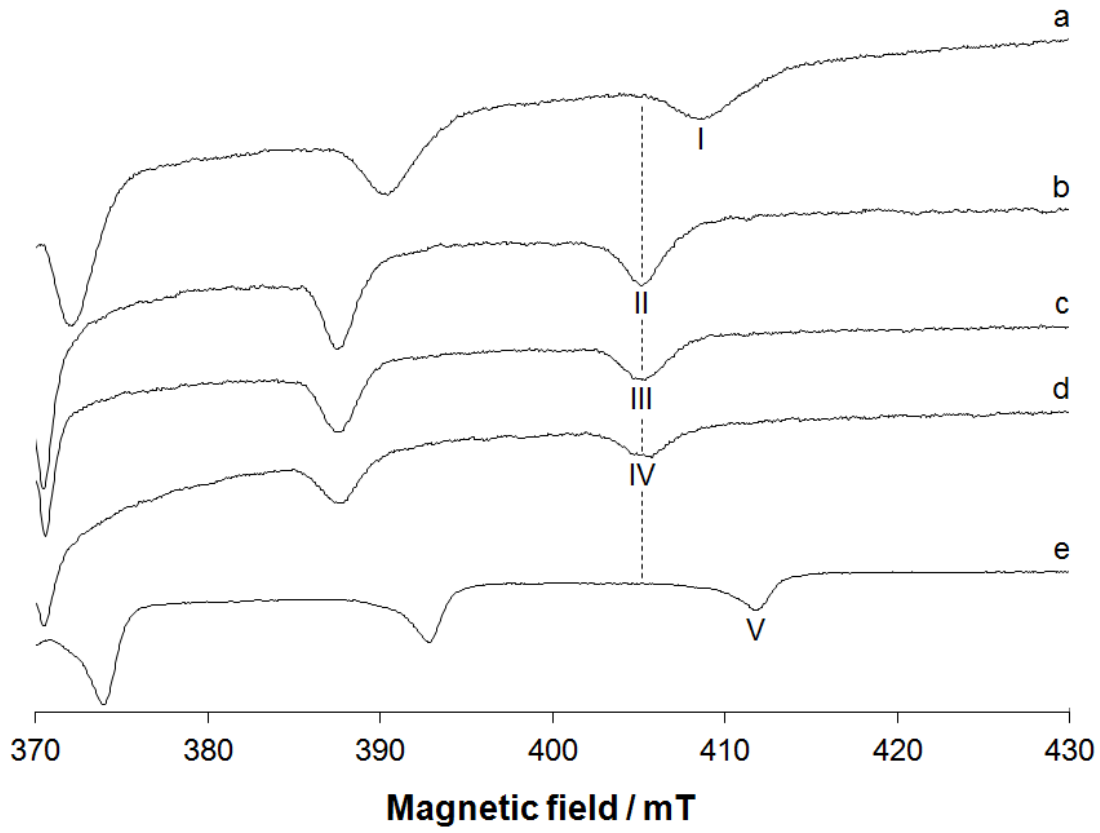

Figure 8. High field region of the X-band anisotropic EPR spectra recorded at 120 K at pH 7.4 in the system containing: a) $V^{IV}O^{2+}$/HSA 4/1 ($V^{IV}O^{2+}$ 1.0 × 10^{-3} M); b) $V^{IV}O^{2+}$/Me_2phen/HSA 4/8/1

($V^{IV}O^{2+}$ 1.0 × 10^{-3} M); c) $V^{IV}O^{2+}$/Me_2phen/apo-hTf 2/4/1 ($V^{IV}O^{2+}$ 1.0 × 10^{-3} M); d) $V^{IV}O^{2+}$/Me_2phen/holo-hTf 2/4/1 ($V^{IV}O^{2+}$ 1.0 × 10^{-3} M) and e) $V^{IV}O^{2+}$/apo-hTf 2/1 ($V^{IV}O^{2+}$ 1.0 × 10^{-3} M). The M_I = 7/2 resonance of $(VO)_x$(HSA) is indicated with **I**, of VO–Me_2phen–HSA with **II**, of VO–Me_2phen–apo-hTf with **III**, of VO–Me_2phen–holo-hTf with **IV**, and (VO)(apo-hTf)/$(VO)_2$(apo-hTf) with **V**. The M_I = 7/2 resonance of VO–Me_2phen–Protein is also denoted by the dotted line.

3.4. Ternary system $V^{IV}O$/Me_2phen/Hb

The interaction with hemoglobin of V compounds with stoichiometry VOL or VOL_2 depends on the presence of a water ligand in the equatorial plane which could be replaced by an amino acid residue of the protein: for example, *cis*-[VO(maltolato)(H_2O)] or [VO(1,2-dimethyl-3-hydroxy-4(1*H*)-pyridinonato)$_2$(H_2O)] form *cis*-VOL_2(Hb) species upon the replacement of water by an equatorial His-N, whereas [VO(6-methylpicolinato)(OH)(H_2O)] gives VOL(Hb)(OH);[30a, 30b] in contrast with [VO(acetylacetonato)$_2$], which is square pyramidal with not available equatorial sites and is thermodynamically stable, no interaction occurs.[30a]

Anisotropic EPR spectrum recorded at pH 7.4 on the ternary system $V^{IV}O^{2+}$/Me_2phen/Hb (Figure S16 of ESI) exhibits signals with g_z 1.953 and A_z 158.7 × 10^{-4} cm^{-1} at ratio 2/4/1 (trace b of Figure S16) and with g_z 1.953 and A_z 160.3 × 10^{-4} cm^{-1} at ratio 2/10/1 (trace c of Figure S16). Analogous shift with varying the molar ratio was observed for HSA (cfr. with Figure 7). Thus, it is probable that, as noticed in those systems, the ratio Me_2phen/$V^{IV}O^{2+}$ influences the relative amount of VO(Me_2phen)(Hb)(OH) and/or *cis*-VO(Me_2phen)$_2$(Hb) and/or a general species with bidentate coordination of hemoglobin (Scheme 5, structures d-g). Therefore, similarly to what was done for HSA and hTf, the EPR transitions are attributed to a mixed complex VO–Me_2phen–Hb.

It is noteworthy that the resonances of the two Hb sites, named β and γ, in which $V^{IV}O^{2+}$ is unspecifically bound to His-N and Asp/Glu-COO^- residues are not revealed (**III** and **IV** in Figure S16).

3.5. Uptake by the red blood cells and redox stability in cell culture medium

The uptake of Metvan by red blood cells at pH 7.4 was monitored by EPR and UV-Vis spectroscopy according to the procedure recently published.[30a, 30b] In the analysis of the results, it must be remembered that the species formed by $V^{IV}O^{2+}$ ion inside the erythrocytes upon the replacement of both L^- by the cytosol bioligands are the same as with vanadate(V), $H_2V^VO_4^-$, because this latter is reduced to $V^{IV}O^{2+}$ by glutathione and subsequently complexed. If the erythrocytes are incubated with V^V, four complexes are revealed (**III-VI** in Figure 9). Two of the four species are formed by Hb ($(VO)Hb^{\beta}$ and $(VO)Hb^{\gamma}$, **IV** and **V** in Figure 9), with the probable V binding by His-N and Asp/Glu-COO donors.[30a] The identity of the other two compounds (**III** and **VI** in Figure 9) has not still proved and they were denoted generally as $VO(L_1,L_2)$ and $VO(L_3,L_4)$ where L_1, L_2, L_3 and L_4 are unidentified erythrocyte bioligands (they may be proteins of the cytosol such as hemoglobin or of cell membrane, and/or low molecular mass bioligands such as ATP, ADP, GSH, lactate, amino acids, sialic acid, 2,3-diphosphoglycerate, urea and sugars). The high g_z value for $VO(L_1,L_2)$ (1.959) would suggest the S coordination to V^{IV}, indicating the interaction of $V^{IV}O^{2+}$ with –SH groups of GSH and/or membrane proteins.[30a, 30b, 63]

The erythrocytes were incubated at 37 °C with a solution containing *cis*-$[VO(Me_2phen)_2(OH)]^+$ (the species existing at the physiological pH in the system $V^{IV}O^{2+}$/Me_2phen) to obtain a final concentration of V complex in the extracellular medium of 5.0×10^{-4} M. After 60, 120 and 180 min of incubation, the red blood cells were separated by centrifugation and EPR spectra were recorded at 120 K on the erythrocyte lysates. Unfortunately, for this system, the spectrophotometric determination of the extracellular V concentration, recently discussed in the literature (based on the oxidation of a $V^{IV}O$ species to the anionic V^V $[V^VO_2(PAR)]^-$ which absorbs at 542 nm,[30a, 30b] see section 2.5) cannot be applied because the absorbance of the extracellular medium is greater than that of a solution containing V 5.0×10^{-4} M (i. e. when all V is in the extracellular medium). This is due to the partial breakage of the erythrocytes caused by the $V^{IV}O$ complex, which has as consequence that Fe^{II} is released in the extracellular medium and its absorption at 542 nm adds to that of V; considering the well-known cytotoxicity of phenanthroline derivatives,[64] the damage to the red blood cell membrane could be induced by the free ligand Me_2phen.

When the erythrocytes are incubated with *cis*-$[VO(Me_2phen)_2(OH)]^+$, this latter can distribute between extra- and intracellular medium.[25b, 30, 38] Inside the red blood cells, ligand exchange and/or redox reactions are possible. EPR spectra recorded as a function of the time are shown in traces c and d of Figure 9. An increase of the spectral intensity in the time range 60-180 min was observed (cfr. traces c and d), suggesting that Metvan, in the form of *cis*-$[VO(Me_2phen)_2(OH)]^+$, crosses the membrane and reaches the cytosol. The EPR intensity increases more quickly in the first hour and then gets slower at 2 and 3 h (Figure 10).

Concerning the complexes formed in the cytosol, it is noteworthy that the ternary complex VO–Me_2phen–Hb (**II** in Figure 9) is the major species. Taking into account what was discussed in the section "Ternary system $V^{IV}O$/Me_2phen/Hb", it may be stated that *cis*-$[VO(Me_2phen)_2(OH)]^+$ crosses the red blood cell membrane and in the cytosol hemoglobin replaces OH^- ion with a surface His-N donor. The other resonances revealed (indicated with **IV** and **V**) can be ascribed to the sites β and γ of Hb ($(VO)Hb^{\beta}$ and $(VO)Hb^{\gamma}$). Overall, the results demonstrated that the thermodynamic stability of *cis*-$[VO(Me_2phen)_2(OH)]^+$ is so high that the two ligands remain bound to V and the replacement reactions of Me_2phen are negligible. Only Hb seems to be able to give a small amount of binary species with $V^{IV}O^{2+}$ ion.

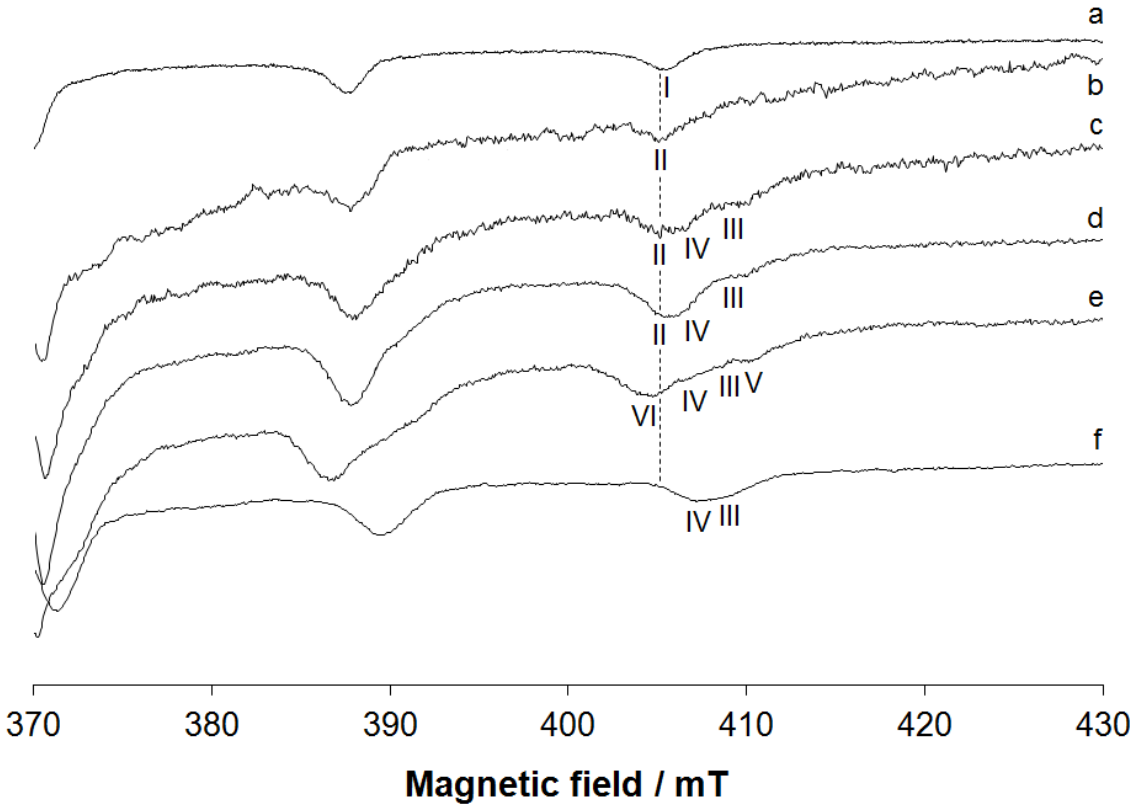

Figure 9. High field region of the X-band anisotropic EPR spectra recorded at 120 K at pH 7.4 in the system containing: a) $V^{IV}O^{2+}$/Me_2phen/MeIm 1/2/4 ($V^{IV}O^{2+}$ 1.0 × 10^{-3} M); b) $V^{IV}O^{2+}$/Me_2phen/Hb 2/4/1 ($V^{IV}O^{2+}$ 6.2 × 10^{-4} M); c) lysate samples of erythrocyte incubated with *cis*-$[VO(Me_2phen)_2(OH)]^+$ for 60 min; d) lysate samples of erythrocyte incubated with *cis*-$[VO(Me_2phen)_2(OH)]^+$ for 180 min; e) lysate samples of erythrocyte incubated with vanadate(V) for 1 h and f) $V^{IV}O^{2+}$/Hb 2/1 ($V^{IV}O^{2+}$ 6.2 ×10^{-4} M). The M_I = 7/2 resonance of VO–Me_2phen–MeIm is indicated with **I**, of VO–Me_2phen–Hb with **II**, of the sites β and γ of Hb

((VO)Hb$^{\beta}$ and (VO)Hb$^{\gamma}$) with **III** and **IV** and of VO(L_3,L_4) and VO(L_1,L_2) with **V** and **VI**. The M_I = 7/2 resonance of VO–Me_2phen–Hb is also denoted by the dotted line.

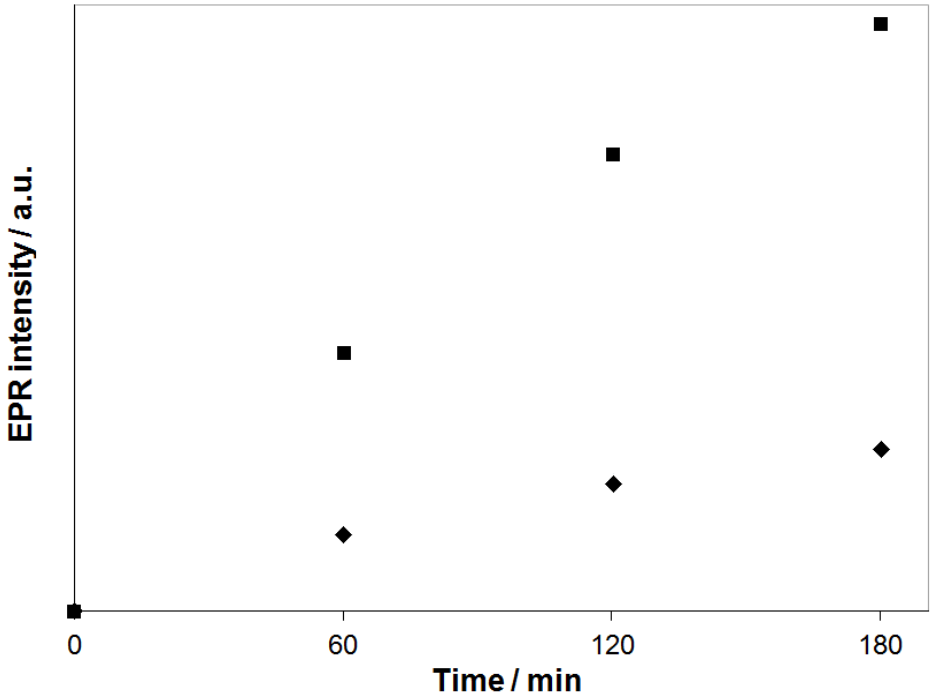

Figure 10. Time dependence of the EPR intensity (in arbitrary units) in lysate samples of erythrocyte incubated with *cis*-[VO(Me_2phen)$_2$(OH)]$^+$. With the rhombi and squares the intensity of the parallel M_I = -5/2 and perpendicular M_I = 5/2 resonances are, respectively, indicated. It must be noticed that the experimental spectral intensity of the perpendicular M_I = 5/2 resonance is larger than the parallel M_I = -5/2 and, for this reason, the values reported along the *y* axis are different.

Crans and Lay reported that the solubilization of Metvan in cell culture medium led to rapid oxidation of V^{IV} to V^{V} and release of the free ligand, to which the pharmacological activity should be attributed.[18, 29] To shed light on this possible oxidation process and eventually confirm the results of Crans and Lay, experiments in RPMI cell culture medium were carried out at 37 °C with a 4.54 × 10^{-4} M solution of Metvan. EPR intensity of V^{IV} signals were monitored as a function of time and reported in Figure 11. To make possible the comparison among the various spectra, the intensity at t = 0 min was set equal to 100%. As it can be observed, the oxidation is not very fast and after 5 hours the intensity of EPR signals is still 40% of that initial value. In the times revealed by Sakurai and co-workers for disappearance of V^{IV} compounds in circulating blood (5 min in rats treated with $VOSO_4$, 8 min in rats treated with [VO(picolinato)$_2$(H_2O)] and more than 30 min in those treated

with [VO(5-iodopicolinato)$_2$] [65]), and at the concentrations used in these experiments the oxidation can be considered partial and part of Metvan could reach the target cells in the initial administered form.

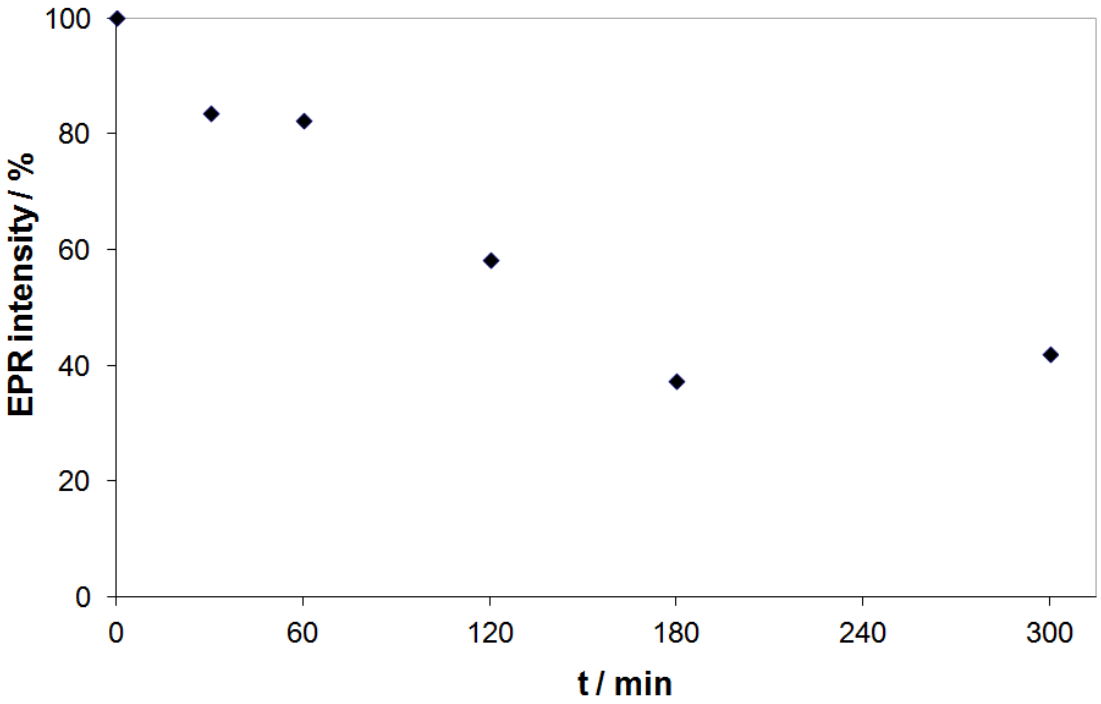

Figure 11. Percent intensity of the EPR signal of the Metvan (4.54×10^{-4} M) measured as a function of time at 37 °C.

3.6 Speciation of Metvan in the blood

In spite of the high multitargeted anti-cancer activity of Metvan, few data are available on the speciation under physiological conditions. On the lack of information on its speciation and thermodynamic/redox stability, indeed, depend the transport in the blood and the active form which reaches the target organs. Rehder wrote that Metvan is not likely to survive *in vivo* conditions and that the active species could be a simple $V^{IV}O^{2+}$ compound.[28] More recently, Crans and Lay observed that the oxidation of Metvan in cell culture medium could be very rapid; this would result in the release of Me_2phen which may be the species with the pharmacological action.[18, 29]

Another important aspect is represented by the possible oral administration. As it has been pointed out in the literature, when internalized orally V compounds are subjected to extreme pH

values (particularly in the stomach where pH is ca. 2);[7b] under these conditions, Metvan cannot survive and it transforms to mono-chelated $[VO(Me_2phen)(H_2O)_3]^{2+}$ and, in part, to aquaion $[VO(H_2O)_5]^{2+}$ (see Figure 1). To overcome the potentially 'destructive' effects of the strong acidity of stomach drug encapsulation should be used.[7b] With this expedient, after the absorption in the small intestine, the intact $[VO(Me_2phen)_2(SO_4)]$ will enter the blood stream, where at pH 7.4 it will become $[VO(Me_2phen)_2(OH)]^+$; this latter species will react with the proteins of the serum and l.m.m. components. Moreover, it can interact with erythrocytes and can passively diffuse into these latter, decreasing the amount present in the serum. The final fate of Metvan depends mainly on the V concentration in the serum. The concentration for healthy humans is in the range 0.2-15 nM,[7e, 66] whereas upon oral treatment with a potential V drug it increases to 1-10 μM for humans [3e, 4, 22a], and to 40-60 μM in rats treated with BMOV or BEOV.[67]

Model calculations based on the thermodynamic stability constants of the species revealed in the systems containing $V^{IV}O^{2+}$, Me_2phen and proteins/l.m.m. ligands were carried out to establish the chemical form of $V^{IV}O^{2+}$ in the concentration range from 1 nM to 1 mM (for proteins the logβ of $[VO(Me_2phen)(MeIm)(OH)]^+$ and $[VO(Me_2phen)_2(MeIm)]^{2+}$, Table 1, and the concentrations reported by Harris and Hamilton [68, 69] were considered for the calculations). The results are displayed in Figure 12.

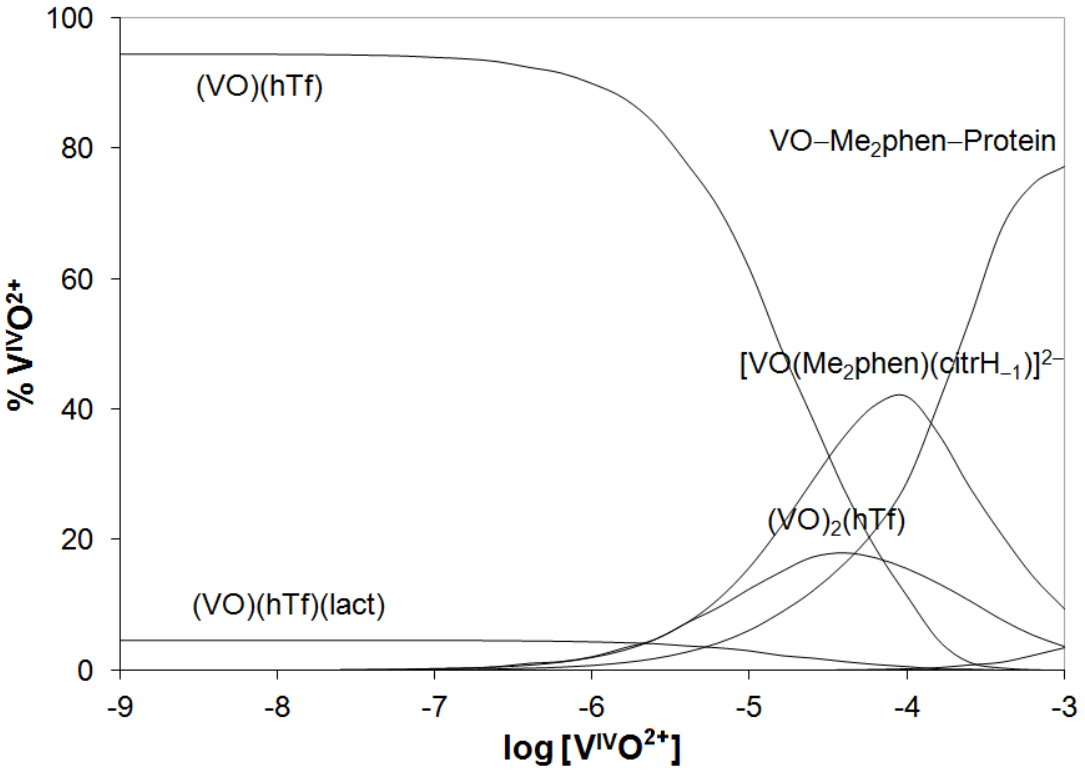

Figure 12. Calculated speciation in the blood serum for Metvan at pH 7.4. $V^{IV}O^{2+}$/Me_2phen molar ratio was 1/2. The concentration of the blood bioligands was taken from refs. [68-69].

It can be observed that, when the V concentration is larger than 50 μM, the major species at pH 7.4 should be $[VO(Me_2phen)(citrH_{-1})]^{2-}$ and the mixed complexes with the proteins indicated with VO–Me_2phen–Protein (their sum is reported in Figure 12). $VO(Me_2phen)_2$(holo-hTf) can be taken up by the target cells since holo-hTf assumes the closed conformation and the metal species can be recognized by the transferrin receptor (TfR) and internalized in the receptor-mediated endocytosis.[7b, 70]

For V concentrations of 10 μM or lower, the predominant species becomes (VO)(hTf), where $V^{IV}O^{2+}$ occupies one of the binding sites of transferrin in the N- or C-terminal region of protein, which should reach percentages close to 95% for concentrations below 1 μM; only a small amount of the mixed complex (VO)(hTf)(lact) is expected (< 5%, see Figure 12). In other words, the reaction $VO(Me_2phen)_2$ + hTf → (VO)(hTf) + 2 Me_2phen takes place. The formation of (VO)(hTf) could also slow down the oxidation of V^{IV} to V^{V}.[71] In normal plasma, the distribution of iron in hTf is approximately 26.7% Fe_2(hTf), 22.9% Fe_N(hTf), 11.2% Fe_C(hTf) and 39.2% apo-hTf,[72] so the species (Fe_N,VO_C)(hTf)/(VO_N,Fe_C)(hTf) and $(VO)_2$(hTf) can be formed. In the first ones ((Fe_N,VO_C)(hTf)/(VO_N,Fe_C)(hTf)) the conformation of hTf is certainly closed and they can be internalized by receptor-mediated endocytosis; concerning the second one ($(VO)_2$(hTf)), it is not clear if with $V^{IV}O^{2+}$ the closing of the hTf conformation can occur, even if Costa-Pessoa and co-workers demonstrated through urea gel electrophoresis experiments that this is very probable.[22f]
Once inside the cell, the conversion of $V^{IV}O$ to $V^{V}O/V^{V}O_2$ (at least partially), proposed by Crans and Lay,[18, 29] must be considered. Even if a redox cycle has not been still demonstrated and the relative amount of V^{IV} and V^{V} species is not known, an equilibrium between the two oxidation states in the cellular environment can be established.[19, 28, 73] The possible key steps of the V antitumor effects appear to be the inhibition of cellular tyrosine phosphatases and/or the generation of ROS.[7b, 7c, 8d, 8e] In this regard it was highlighted that also hydrolytic V^{IV} complexes, structurally similar to the tetrahedral species of V^{V} such as $[V^{V}O_2(OH)_2]^-$ (≡ $H_2V^{V}O_4^-$), may inhibit the phosphatases.[20, 74, 75] This proposal is consistent with the observation that also aqueous V^{IV} acts as inhibitor of several phosphatases, and in some cases it is as effective as V^{V}.[74, 76] Considering that $V^{IV}O$ is able to initiate Fenton-like reactions,[77] it is plausible to state that both $V^{IV}O$ and $V^{V}O/V^{V}O_2$ may contribute to the pharmacological activity and their effects may be synergic. Finally, as pointed out by Lay and Crans,[18, 29] it must be noticed that also the action of free ligand Me_2phen, formed in

aqueous solution for V concentrations lower than 50 μM and whose the cytotoxic activity is well documented,[64] could add to that of V^{IV}/V^{V} species.

Concerning the distribution of V^{IV} species between blood serum and erythrocytes, the ratio depends on the binding to the blood bioligands and on rates of influx and efflux across the erythrocyte membrane.[71] It has been suggested that in mammals the distribution of vanadium between plasma and erythrocytes is in the range 70:30-95:5 and does not seem to be dependent on the chemical form initially present.[71, 78] The data of this study that Metvan can cross the membrane, forming in the cytosol VO–Me_2phen–Hb, in particular when the V concentration is enough large (> 50 μM).

On the basis of the results discussed in this section, the biotransformation of Metvan in the blood as a function of V concentration and the possible active species are shown in Scheme 6.

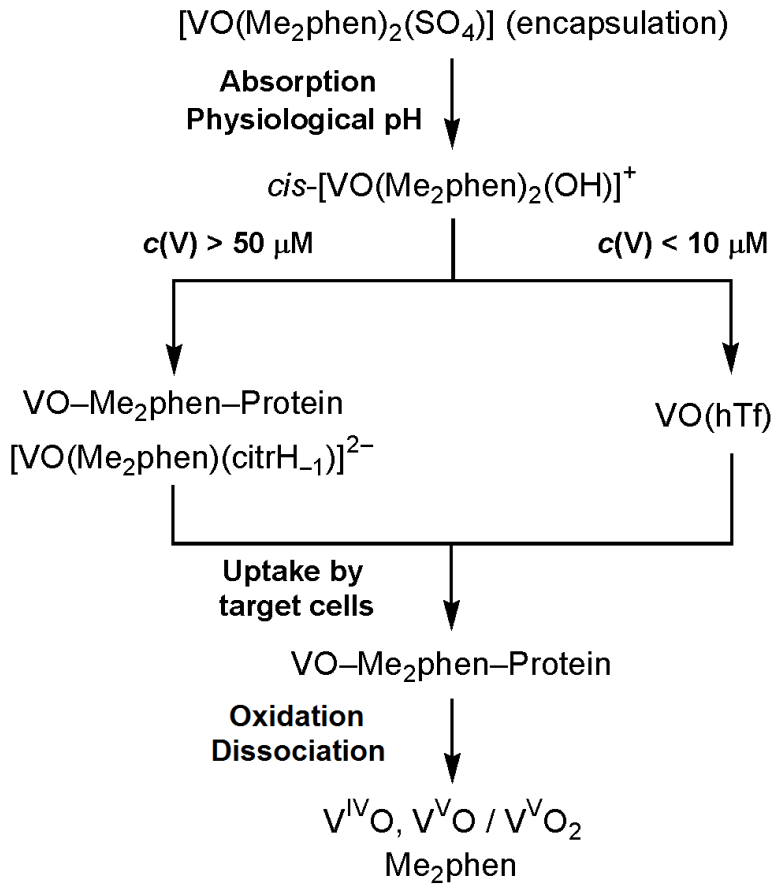

Scheme 6. Possible biotransformations of Metvan in the blood and cells after the administration.

4. Conclusions

One of the most promising potential applications of vanadium compounds in medicine is as anti-tumor drugs.[8] The compound $[V^{IV}O(Me_2phen)_2(SO_4)]$, also known as Metvan, was identified as one of the most potent anti-cancer V compounds with apoptosis-inducing activity. It is effective against several tumor cell lines and its activity against cisplatin-resistant ovarian and testicular cancer appears to be very promising.[8e, 12-13, 14] Despite that it was immediately identified as one of the most promising multitargeted anti-cancer V compounds, no development on the possible medical experimentation was carried out after the first reports in the literature.[12-13, 14] One of the reason is the lack of information on its speciation in aqueous solution and its thermodynamic stability, which influence the transport in the blood and the final form that reaches the target organs; such a lack of information has hindered, up now, to understand completely the mechanism of action of Metvan, which has been related to the generation of ROS,[7e] or to the interaction with DNA *via* intercalation and π···π interaction.[7c]

The results obtained in this work indicate that the organic ligand Me_2phen can bind the $V^{IV}O^{2+}$ ion also in the physiological pH range and the species *cis*-$[VO(Me_2phen)_2(OH)]^+$, formed at pH 7.4, can interact with the plasma bioligands and red blood cells. $[VO(Me_2phen)_2(OH)]^+$ can react with the serum proteins forming mixed species whose composition can be indicated with the general formulation VO–Me_2phen–Protein; the binding of one His-N or two different amino acid donors is probable. Among the other complexes formed, the ternary species with the tridentate citrate, $[VO(Me_2phen)(citrH_{-1})]^{2-}$, is very important, whereas in the red blood cells VO–Me_2phen–Hb should be the major complex.

These results are in partial contrast with the observation that Metvan should not survive *in vivo* conditions with the consequence that the active species could be a simple V^{IV} species,[28] or the free ligand Me_2phen.[18, 29] As a matter of fact the speciation of Metvan in the blood depends mainly on the V concentration in the serum. When the V concentration is larger than 50 μM, $V^{IV}O^{2+}$ remains bound to Me_2phen and $[VO(Me_2phen)(citrH_{-1})]^{2-}$ and VO–Me_2phen–Protein are the major species. The latter species, when Protein is hTf, can be internalized in the cells, in the receptor-mediated endocytosis. For V concentration lower than 10 μM, the results are in agreement with what predicted by Rehder,[28] and recently by Crans and Lay:[18, 29] the reaction $VO(Me_2phen)_2$ + hTf → (VO)(hTf) + 2 Me_2phen occurs and $V^{IV}O^{2+}$ is taken up by the cells, where the partial conversion of $V^{IV}O$ to $V^{V}O/V^{V}O_2$ may happen. In the cellular environment the active species could be $[V^{V}O_2(OH)_2]^-$ (≡ $H_2V^{V}O_4^-$) and tetrahedral V^{IV} complexes, such as $[V^{IV}O(OH)_3]^-$ (≡ $H_3V^{IV}O_4^-$) or other hydrolytic products. These complexes are potent inhibitors of tyrosine phosphatases and V^{IV} may generate ROS through Fenton-like reaction; therefore, $V^{IV}O$ and $V^{V}O/V^{V}O_2$ may contribute in

synergic mode to the pharmacological activity of Metvan. Finally, as pointed out by Lay and Crans,[18, 29] the effect of free Me_2phen could add to that of V^{IV}/V^{V} species.

We hope that these results could promote new studies on the anti-cancer activity of Metvan and the possible restart of its clinical experimentation. For the next future the study of the interaction with the cellular bioligands, for example actin which plays a significant role in the V accumulation and transport processes within the cells[79], could contribute to give a better picture of the pharmacological action of Metvan.

5. Acknowledgement

This research was supported by Fondazione di Sardegna (FdS15Garribba) and European Union, and co-financed by the European Regional Development Fund under the project GINOP-2.3.2-15-2016-00008. The authors thank Servizio Trasfusionale Aziendale (AOU of Sassari) for providing the blood samples.

References

1. B. Lyonnet, F. Martz and E. Martin, *La Presse Medicale*, 1899, **32**, 191-192.
2. (a) Y. Shechter and S. J. D. Karlish, *Nature*, 1980, **284**, 556-558; (b) Y. Shechter, I. Goldwaser, M. Mironchik, M. Fridkin and D. Gefel, *Coord. Chem. Rev.*, 2003, **237**, 3-11.
3. (a) K. H. Thompson, J. H. McNeill and C. Orvig, *Chem. Rev.*, 1999, **99**, 2561-2572; (b) K. H. Thompson and C. Orvig, *Coord. Chem. Rev.*, 2001, **219–221**, 1033-1053; (c) K. H. Thompson and C. Orvig, in *Met. Ions Biol. Syst.*, eds. H. Sigel and A. Sigel, Marcel Dekker, New York, 2004, vol. 41, pp. 221-252; (d) K. H. Thompson, B. D. Liboiron, G. R. Hanson and C. Orvig, in *Medicinal Inorganic Chemistry*, eds. J. L. Sessler, S. R. Doctrow, T. J. McMurry and S. J. Lippard, American Chemical Society, Washington DC, 2005, vol. 903, ch. 21, pp. 384-399; (e) K. H. Thompson and C. Orvig, *J. Inorg. Biochem.*, 2006, **100**, 1925-1935; (f) H. Sakurai, Y. Yoshikawa and H. Yasui, *Chem. Soc. Rev.*, 2008, **37**, 2383-2392.
4. K. H. Thompson, J. Lichter, C. LeBel, M. C. Scaife, J. H. McNeill and C. Orvig, *J. Inorg. Biochem.*, 2009, **103**, 554-558.
5. J. Costa Pessoa and I. Tomaz, *Curr. Med. Chem.*, 2010, **17**, 3701-3738.
6. K. D. Mjos and C. Orvig, *Chem. Rev.*, 2014, **114**, 4540-4563.
7. (a) D. Gambino, *Coord. Chem. Rev.*, 2011, **255**, 2193-2203; (b) D. Rehder, *Future Med. Chem.*, 2012, **4**, 1823-1837; (c) D. Rehder, in *Interrelations between Essential Metal Ions and Human Diseases*, eds. A. Sigel, H. Sigel and R. K. O. Sigel, Springer Science+Business Media, Dordrecht, 2013, ch. 5, pp. 139-169; (d) M. Aureliano and C. A. Ohlin, *J. Inorg. Biochem.*, 2014, **137**, 123-130; (e) J. Costa Pessoa, S. Etcheverry and D. Gambino, *Coord. Chem. Rev.*, 2015, **301-302**, 24-48; (f) D. Rehder, *Future Med. Chem.*, 2016, **8**, 325-338; (g) D. Rehder, *Inorg. Chim. Acta*, 2017, **455**, 378-389.
8. (a) D. A. Barrio and S. B. Etcheverry, *Curr. Med. Chem.*, 2010, **17**, 3632-3642; (b) A. Bishayee, A. Waghray, M. A. Patel and M. Chatterjee, *Cancer Lett.*, 2010, **294**, 1-12; (c) S. Das, M. Chatterjee, M. Janarthan, H. Ramachandran and M. Chatterjee, in *Vanadium. Biochemical and Molecular Biological Approaches*, ed. H. Michibata, Springer Netherlands, 2012, ch. 8, pp. 163-185; (d) E. Kioseoglou, S. Petanidis, C. Gabriel and A. Salifoglou, *Coord. Chem. Rev.*, 2015, 87-105; (e) A. M. Evangelou, *Crit. Rev. Oncol. Hematol.*, 2002, **42**, 249-265.
9. (a) P. Köpf-Maier and D. Krahl, *Chem.-Biol. Interact.*, 1983, **44**, 317-328; (b) P. Köpf-Maier and H. Köpf, *Chem. Rev.*, 1987, **87**, 1137-1152.

10. B. Gleeson, J. Claffey, M. Hogan, H. Müller-Bunz, D. Wallis and M. Tacke, *J. Organomet. Chem.*, 2009, **694**, 1369-1374.
11. B. Gleeson, A. Deally, H. Müller-Bunz, S. Patil and M. Tacke, *Aust. J. Chem.*, 2010, **63**, 1514-1520.
12. (a) R. K. Narla, Y. Dong, D. Klis and F. M. Uckun, *Clin. Cancer Res.*, 2001, **7**, 1094-1101; (b) R. K. Narla, Y. Dong, D. Klis and F. M. Uckun, *Clin. Cancer Res.*, 2001, **7**, 2124-2133.
13. O. J. Cruz and F. M. Uckun, *Expert Opin. Invest. Drugs*, 2002, **11**, 1829-1836.
14. Y. Dong, R. K. Narla, E. Sudbeck and F. M. Uckun, *J. Inorg. Biochem.*, 2000, **78**, 321-330.
15. T. Scior, J. A. Guevara-Garcia, Q.-T. Do, P. Bernard and S. Laufer, *Curr. Med. Chem.*, 2016, **23**, 2874-2891.
16. I. E. Leon, P. Diez, S. B. Etcheverry and M. Fuentes, *Metallomics*, 2016, **8**, 739-749.
17. J.-X. Wu, Y.-H. Hong and X.-G. Yang, *JBIC, J. Biol. Inorg. Chem.*, 2016, **21**, 919-929.
18. A. Levina, D. C. Crans and P. A. Lay, *Coord. Chem. Rev.*, 2017, DOI: 10.1016/j.ccr.2017.01.002.
19. K. A. Doucette, K. N. Hassell and D. C. Crans, *J. Inorg. Biochem.*, 2016, **165**, 56-70.
20. Y. Yoshikawa, H. Sakurai, D. C. Crans, G. Micera and E. Garribba, *Dalton Trans.*, 2014, **43**, 6965-6972.
21. (a) D. Sanna, G. Micera and E. Garribba, *Inorg. Chem.*, 2009, **48**, 5747-5757; (b) D. Sanna, G. Micera and E. Garribba, *Inorg. Chem.*, 2010, **49**, 174-187; (c) D. Sanna, P. Buglyó, G. Micera and E. Garribba, *JBIC, J. Biol. Inorg. Chem.*, 2010, **15**, 825-839; (d) D. Sanna, G. Micera and E. Garribba, *Inorg. Chem.*, 2011, **50**, 3717-3728; (e) D. Sanna, L. Biro, P. Buglyo, G. Micera and E. Garribba, *Metallomics*, 2012, **4**, 33-36; (f) D. Sanna, V. Ugone, G. Micera and E. Garribba, *Dalton Trans.*, 2012, **41**, 7304-7318; (g) D. Sanna, L. Bíró, P. Buglyó, G. Micera and E. Garribba, *J. Inorg. Biochem.*, 2012, **115**, 87-99; (h) D. Sanna, G. Micera and E. Garribba, *Inorg. Chem.*, 2013, **52**, 11975-11985; (i) T. Koleša-Dobravc, E. Lodyga-Chruscinska, M. Symonowicz, D. Sanna, A. Meden, F. Perdih and E. Garribba, *Inorg. Chem.*, 2014, **53**, 7960-7976.
22. (a) G. R. Willsky, A. B. Goldfine, P. J. Kostyniak, J. H. McNeill, L. Q. Yang, H. R. Khan and D. C. Crans, *J. Inorg. Biochem.*, 2001, **85**, 33-42; (b) B. D. Liboiron, K. H. Thompson, G. R. Hanson, E. Lam, N. Aebischer and C. Orvig, *J. Am. Chem. Soc.*, 2005, **127**, 5104-5115; (c) T. Jakusch, J. C. Pessoa and T. Kiss, *Coord. Chem. Rev.*, 2011, **255**, 2218-2226; (d) I. Correia, T. Jakusch, E. Cobbinna, S. Mehtab, I. Tomaz, N. V. Nagy, A. Rockenbauer, J. Costa Pessoa and T. Kiss, *Dalton Trans.*, 2012, **41**, 6477-6487; (e) J. B. Vincent and S. Love, *Biochim. Biophys. Acta, Gen. Subj.*, 2012, **1820**, 362-378; (f) S. Mehtab, G. Gonçalves, S. Roy, A. I.

Tomaz, T. Santos-Silva, M. F. A. Santos, M. J. Romão, T. Jakusch, T. Kiss and J. Costa Pessoa, *J. Inorg. Biochem.*, 2013, **121**, 187-195; (g) G. Gonçalves, A. I. Tomaz, I. Correia, L. F. Veiros, M. M. C. A. Castro, F. Avecilla, L. Palacio, M. Maestro, T. Kiss, T. Jakusch, M. H. V. Garcia and J. Costa Pessoa, *Dalton Trans.*, 2013, **42**, 11841-11861; (h) M. F. A. Santos, I. Correia, A. R. Oliveira, E. Garribba, J. C. Pessoa and T. Santos-Silva, *Eur. J. Inorg. Chem.*, 2014, 3293-3297; (i) J. Costa Pessoa, E. Garribba, M. F. A. Santos and T. Santos-Silva, *Coord. Chem. Rev.*, 2015, **301-302**, 49-86.

23. A. Levina and P. A. Lay, *Chem. Asian J.* , 2017, DOI: 10.1002/asia.201700463.
24. T. Jakusch and T. Kiss, *Coord. Chem. Rev.*, 2017, DOI: 10.1016/j.ccr.2017.04.007.
25. (a) D. Sanna, V. Ugone, G. Micera, T. Pivetta, E. Valletta and E. Garribba, *Inorg. Chem.*, 2015, **54**, 8237-8250; (b) D. Sanna, M. Serra, V. Ugone, L. Manca, M. Pirastru, P. Buglyo, L. Biro, G. Micera and E. Garribba, *Metallomics*, 2016, **8**, 532-541.
26. I. G. Macara, K. Kustin and L. C. Cantley Jr, *Biochim. Biophys. Acta, Gen. Subj.*, 1980, **629**, 95-106.
27. P. C. Wilkins, M. D. Johnson, A. A. Holder and D. C. Crans, *Inorg. Chem.*, 2006, **45**, 1471-1479.
28. D. Rehder, *Bioinorganic Vanadium Chemistry*, John Wiley & Sons, Ltd, Chichester, 2008.
29. M. Le, O. Rathje, A. Levina and P. A. Lay, *JBIC, J. Biol. Inorg. Chem.*, 2017, DOI: 10.1007/s00775-017-1453-4.
30. (a) D. Sanna, M. Serra, G. Micera and E. Garribba, *Inorg. Chem.*, 2014, **53**, 1449-1464; (b) D. Sanna, M. Serra, G. Micera and E. Garribba, *Inorg. Chim. Acta*, 2014, **420**, 75-84; (c) D. Sanna, D. Fabbri, M. Serra, P. Buglyó, L. Bíró, V. Ugone, G. Micera and E. Garribba, *J. Inorg. Biochem.*, 2015, **147**, 71-84; (d) D. Sanna, V. Ugone, L. Pisano, M. Serra, G. Micera and E. Garribba, *J. Inorg. Biochem.*, 2015, **153**, 167-177.
31. A. Levina, A. I. McLeod, S. J. Gasparini, A. Nguyen, W. G. M. De Silva, J. B. Aitken, H. H. Harris, C. Glover, B. Johannessen and P. A. Lay, *Inorg. Chem.*, 2015, **54**, 7753-7766.
32. J. Gätjens, B. Meier, Y. Adachi, H. Sakurai and D. Rehder, *Eur. J. Inorg. Chem.*, 2006, 3575-3585.
33. H. M. Irving, M. G. Miles and L. D. Pettit, *Anal. Chim. Acta*, 1967, **38**, 475-488.
34. L. Zékány and I. Nagypál, in *Computation Methods for the Determination of Formation Constants*, ed. D. J. Leggett, Plenum Press, New York, 1985, pp. 291-353.
35. C. W. Davies, *J. Chem. Soc.*, 1938, 2093-2098.
36. A. Komura, M. Hayashi and H. Imanaga, *Bull. Chem. Soc. Jpn.*, 1977, **50**, 2927-2931.

37. L. F. Vilas Boas and J. Costa Pessoa, in *Comprehensive Coordination Chemistry*, eds. G. Wilkinson, R. D. Gillard and J. A. McCleverty, Pergamon Press, Oxford, 1985, vol. 3, pp. 453-583.
38. T. C. Delgado, A. I. Tomaz, I. Correia, J. Costa Pessoa, J. G. Jones, C. F. G. C. Geraldes and M. M. C. A. Castro, *J. Inorg. Biochem.*, 2005, **99**, 2328-2339.
39. M. J. C. Taylor and J. F. van Staden, *Analyst*, 1994, **119**, 1263-1276.
40. F. Genç, K. Gavazov and M. Türkyilmaz, *Cent. Eur. J. Chem.*, 2010, **8**, 461-467.
41. D. Sanna, E. Garribba and G. Micera, *J. Inorg. Biochem.*, 2009, **103**, 648-655.
42. M. J. Frisch, G. W. Trucks, H. B. Schlegel, G. E. Scuseria, M. A. Robb, J. R. Cheeseman, J. A. Montgomery, Jr., T. Vreven, K. N. Kudin, J. C. Burant, J. M. Millam, S. S. Iyengar, J. Tomasi, V. Barone, B. Mennucci, M. Cossi, G. Scalmani, N. Rega, G. A. Petersson, H. Nakatsuji, M. Hada, M. Ehara, K. Toyota, R. Fukuda, J. Hasegawa, M. Ishida, T. Nakajima, Y. Honda, O. Kitao, H. Nakai, M. Klene, X. Li, J. E. Knox, H. P. Hratchian, J. B. Cross, C. Adamo, J. Jaramillo, R. Gomperts, R. E. Stratmann, O. Yazyev, A. J. Austin, R. Cammi, C. Pomelli, J. W. Ochterski, P. Y. Ayala, K. Morokuma, G. A. Voth, P. Salvador, J. J. Dannenberg, V. G. Zakrzewski, S. Dapprich, A. D. Daniels, M. C. Strain, O. Farkas, D. K. Malick, A. D. Rabuck, K. Raghavachari, J. B. Foresman, J. V. Ortiz, Q. Cui, A. G. Baboul, S. Clifford, J. Cioslowski, B. B. Stefanov, G. Liu, A. Liashenko, P. Piskorz, I. Komaromi, R. L. Martin, D. J. Fox, T. Keith, M. A. Al-Laham, C. Y. Peng, A. Nanayakkara, M. Challacombe, P. M. W. Gill, B. Johnson, W. Chen, M. W. Wong, C. Gonzalez and J. A. Pople, *Gaussian 03, revision C.02*, Gaussian, Inc., Wallingford, CT, 2004.
43. (a) F. Neese, *Wiley Interdisciplinary Reviews: Computational Molecular Science*, 2012, **2**, 73-78; (b) F. Neese, *ORCA - An Ab Initio, DFT and Semiempirical Program Package, Version 3.0*, Max-Planck-Institute for Chemical Energy Conversion, Mülheim a. d. Ruhr, 2013.
44. (a) M. Bühl and H. Kabrede, *J. Chem. Theory Comput.*, 2006, **2**, 1282-1290; (b) M. Bühl, C. Reimann, D. A. Pantazis, T. Bredow and F. Neese, *J. Chem. Theory Comput.*, 2008, **4**, 1449-1459.
45. G. Micera and E. Garribba, *Int. J. Quantum Chem.*, 2012, **112**, 2486-2498.
46. (a) G. Micera, V. L. Pecoraro and E. Garribba, *Inorg. Chem.*, 2009, **48**, 5790-5796; (b) G. Micera and E. Garribba, *Eur. J. Inorg. Chem.*, 2010, 4697-4710; (c) G. Micera and E. Garribba, *Eur. J. Inorg. Chem.*, 2011, 3768-3780; (d) D. Sanna, K. Varnágy, S. Timári, G. Micera and E. Garribba, *Inorg. Chem.*, 2011, **50**, 10328-10341; (e) D. Sanna, P. Buglyó, L. Bíró, G. Micera and E. Garribba, *Eur. J. Inorg. Chem.*, 2012, 1079-1092; (f) D. Sanna, P. Buglyo, A. I. Tomaz, J. C. Pessoa, S. Borovic, G. Micera and E. Garribba, *Dalton Trans.*,

2012, **41**, 12824-12838; (g) L. Pisano, K. Varnagy, S. Timári, K. Hegetschweiler, G. Micera and E. Garribba, *Inorg. Chem.*, 2013, **52**, 5260-5272; (h) D. Sanna, K. Várnagy, N. Lihi, G. Micera and E. Garribba, *Inorg. Chem.*, 2013, **52**, 8202-8213; (i) E. Lodyga-Chruscinska, A. Szebesczyk, D. Sanna, K. Hegetschweiler, G. Micera and E. Garribba, *Dalton Trans.*, 2013, **42**, 13404-13416.

47. (a) S. Gorelsky, G. Micera and E. Garribba, *Chem.–Eur. J.*, 2010, **16**, 8167-8180; (b) G. Micera and E. Garribba, *J. Comput. Chem.*, 2011, **32**, 2822-2835.
48. L. Gasque, G. Medina, L. Ruiz-Ramírez and R. Moreno-Esparza, *Inorg. Chim. Acta*, 1999, **288**, 106-111.
49. T. W. Duma and R. D. Hancock, *J. Coord. Chem.*, 1994, **31**, 135-146.
50. (a) E. Lodyga-Chruscinska, E. Garribba, G. Micera and A. Panzanelli, *J. Inorg. Biochem.*, 1999, **75**, 225-232; (b) E. Kiss, K. Petrohan, D. Sanna, E. Garribba, G. Micera and T. Kiss, *Polyhedron*, 2000, **19**, 55-61; (c) E. Kiss, E. Garribba, G. Micera, T. Kiss and H. Sakurai, *J. Inorg. Biochem.*, 2000, **78**, 97-108; (d) P. Buglyo, E. Kiss, I. Fabian, T. Kiss, D. Sanna, E. Garribba and G. Micera, *Inorg. Chim. Acta*, 2000, **306**, 174-183; (e) P. Buglyo, T. Kiss, E. Kiss, D. Sanna, E. Garribba and G. Micera, *J. Chem. Soc., Dalton Trans.*, 2002, 2275-2282; (f) M. Rangel, A. Leite, M. J. Amorim, E. Garribba, G. Micera and E. Lodyga-Chruscinska, *Inorg. Chem.*, 2006, **45**, 8086-8097; (g) E. Lodyga-Chruscinska, G. Micera and E. Garribba, *Inorg. Chem.*, 2011, **50**, 883-899.
51. D. N. Chasteen, in *Biological Magnetic Resonance*, eds. L. J. Berliner and J. Reuben, Plenum Press, New York, 1981, vol. 3, ch. 2, pp. 53-119.
52. T. S. Smith II, R. LoBrutto and V. L. Pecoraro, *Coord. Chem. Rev.*, 2002, **228**, 1-18.
53. E. Garribba, E. Lodyga-Chruscinska, G. Micera, A. Panzanelli and D. Sanna, *Eur. J. Inorg. Chem.*, 2005, 1369-1382.
54. G. Micera and E. Garribba, *Dalton Trans.*, 2009, 1914-1918.
55. V. B. Di Marco and G. G. Bombi, *Mass Spectrom. Rev.*, 2006, **25**, 347-379.
56. L. E. Sojo, N. Chahal and B. O. Keller, *Rapid Commun. Mass Spectrom.*, 2014, **28**, 2181-2190.
57. M. P. Waller and M. Bühl, *J. Comput. Chem.*, 2007, **28**, 1531-1537.
58. (a) M. L. Munzarová and M. Kaupp, *J. Phys. Chem. B*, 2001, **105**, 12644-12652; (b) F. Neese, *J. Chem. Phys.*, 2003, **118**, 3939-3948; (c) A. C. Saladino and S. C. Larsen, *J. Phys. Chem. A*, 2003, **107**, 1872-1878; (d) C. P. Aznar, Y. Deligiannakis, E. J. Tolis, T. Kabanos, M. Brynda and R. D. Britt, *J. Phys. Chem. A*, 2004, **108**, 4310-4321; (e) A. C. Saladino and S. C. Larsen, *Catal. Today*, 2005, **105**, 122-133.

59. M. Rangel, A. Tamura, C. Fukushima and H. Sakurai, *JBIC, J. Biol. Inorg. Chem.*, 2001, **6**, 128-132.

60. T. S. Smith II, C. A. Root, J. W. Kampf, P. G. Rasmussen and V. L. Pecoraro, *J. Am. Chem. Soc.*, 2000, **122**, 767-775.

61. Y. Gou, J. Qi, J.-P. Ajayi, Y. Zhang, Z. Zhou, X. Wu, F. Yang and H. Liang, *Mol. Pharm.*, 2015, **12**, 3597-3609.

62. J. Costa Pessoa, G. Gonçalves, S. Roy, I. Correia, S. Mehtab, M. F. A. Santos and T. Santos-Silva, *Inorg. Chim. Acta*, 2014, **420**, 60-68.

63. B. Zhang, L. Ruan, B. Chen, J. Lu and K. Wang, *BioMetals*, 1997, **10**, 291-298.

64. (a) A. Mohindru, J. M. Fisher and M. Rabinovitz, *Biochem. Pharmacol.*, 1983, **32**, 3627-3632; (b) A. Kellett, M. O'Connor, M. McCann, O. Howe, A. Casey, P. McCarron, K. Kavanagh, M. McNamara, S. Kennedy, D. D. May, P. S. Skell, D. O'Shea and M. Devereux, *MedChemComm*, 2011, **2**, 579-584; (c) M. McCann, A. L. S. Santos, B. A. da Silva, M. T. V. Romanos, A. S. Pyrrho, M. Devereux, K. Kavanagh, I. Fichtner and A. Kellett, *Toxicol. Res.*, 2012, **1**, 47-54; (d) C. N. David, E. S. Frias, C. C. Elix, K. E. McGovern, A. M. Walker, J. F. Eichler and E. H. Wilson, *ASN Neuro*, 2015, **7**, 1759091415572365 and references therein.

65. T. Takino, H. Yasui, A. Yoshitake, Y. Hamajima, R. Matsushita, J. Takada and H. Sakurai, *JBIC, J. Biol. Inorg. Chem.*, 2001, **6**, 133-142.

66. G. Heinemann and W. Vogt, *Clin. Chem.*, 1996, **42**, 1275-1282.

67. (a) K. H. Thompson, B. D. Liboiron, Y. Sun, K. D. Bellman, I. A. Setyawati, B. O. Patrick, V. Karunaratne, G. Rawji, J. Wheeler, K. Sutton, S. Bhanot, C. Cassidy, J. H. McNeill, V. G. Yuen and C. Orvig, *JBIC, J. Biol. Inorg. Chem.*, 2003, **8**, 66-74; (b) S.-Q. Zhang, X.-Y. Zhong, G.-H. Chen, W.-L. Lu and Q. Zhang, *J. Pharm. Pharmacol.*, 2008, **60**, 99-105.

68. W. R. Harris, *Clin. Chem.*, 1992, **38**, 1809-1818.

69. R. G. Hamilton, *Clin. Chem.*, 1987, **33**, 1707-1725.

70. Á. Dörnyei, S. Marcão, J. Costa Pessoa, T. Jakusch and T. Kiss, *Eur. J. Inorg. Chem.*, 2006, 3614-3621.

71. W. R. Harris, S. B. Friedman and D. Silberman, *J. Inorg. Biochem.*, 1984, **20**, 157-169.

72. (a) J. Williams and K. Moreton, *Biochem. J.*, 1980, **185**, 483-488; (b) B. E. Eckenroth, A. N. Steere, N. D. Chasteen, S. J. Everse and A. B. Mason, *Proc. Natl. Acad. Sci. U. S. A.*, 2011, **108**, 13089-13094.

73. A. S. Tracey, G. R. Willsky and E. S. Takeuchi, *Vanadium: Chemistry, Biochemistry, Pharmacology and Practical Applications*, CRC Press, Boca Raton, FL, 2007.

74. D. C. Crans, J. J. Smee, E. Gaidamauskas and L. Yang, *Chem. Rev.*, 2004, **104**, 849-902.

75. D. Rehder, *Dalton Trans.*, 2013, **42**, 11749-11761.

76. (a) V. Lopez, T. Stevens and R. N. Lindquist, *Arch. Biochem. Biophys.*, 1976, **175**, 31-38; (b) C. Simone, *Ph.D. Thesis*, Colorado State University, 1992.

77. (a) A. J. Carmichael, *FEBS Lett.*, 1990, **261**, 165-170; (b) T. Ozawa and A. Hanaki, *Chem. Pharm. Bull.*, 1989, **37**, 1407-1409; (c) X. Shi, H. Jiang, Y. Mao, J. Ye and U. Saffiotti, *Toxicology*, 1996, **106**, 27-38; (d) D. Sanna, V. Ugone, A. Fadda, G. Micera and E. Garribba, *J. Inorg. Biochem.*, 2016, **161**, 18-26.

78. E. Sabbioni, E. Marafante, L. Amantini, L. Ubertalli and C. Birattari, *Bioinorg. Chem.* , 1978, **8**, 503-515.

79. (a) S. Ramos, M. Manuel, T. Tiago, R. Duarte, J. Martins, C. Gutiérrez-Merino, J. J. G. Moura and M. Aureliano, *J. Inorg. Biochem.*, 2006, **100**, 1734-1743; (b) S. Ramos, R. O. Duarte, J. J. G. Moura and M. Aureliano, *Dalton Trans.*, 2009, 7985-7994; (c) S. Ramos, J. J. G. Moura and M. Aureliano,

J. Inorg. Biochem., 2010, **104**, 1234-1239; (d) S. Ramos, R. M. Almeida, J. J. G. Moura and M. Aureliano, *J. Inorg. Biochem.*, 2011, **105**, 777-783.

Contents Entry

Text

The speciation in aqueous solution and in human blood of Metvan, $[V^{IV}O(Me_2phen)_2(SO_4)]$, a V based anti-tumor drug, was studied. The results suggested that when the V concentration is > 50 μM, $[VO(Me_2phen)(citrH_{-1})]^{2-}$ and the ternary complexes VO–Me_2phen–Protein should be the major species under physiological conditions, while when V concentration is < 10 μM (VO)(hTf) is formed, Me_2phen is lost and in the cells the partial conversion of $V^{IV}O$ to $V^{V}O/V^{V}O_2$ may occur.

Color graphic